



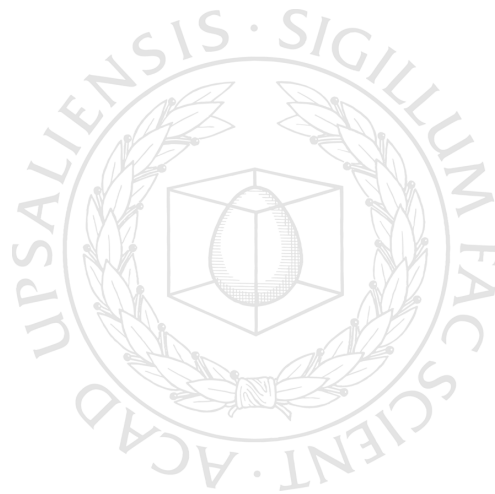
UPPSALA
UNIVERSITET

*Digital Comprehensive Summaries of Uppsala Dissertations
from the Faculty of Science and Technology 81*

Quark Distributions and Charged Higgs Boson Production

Studies of Proton Structure and New Physics

JOHAN ALWALL



ACTA
UNIVERSITATIS
UPSALIENSIS
UPPSALA
2005

ISSN 1651-6214
ISBN 91-554-6316-9
urn:nbn:se:uu:diva-5901

Dissertation at Uppsala University to be publicly examined in Polhemsalen, Ångström Laboratory, Uppsala, Friday, September 23, 2005 at 13:15 for the Degree of Doctor of Philosophy. The examination will be conducted in English.

Abstract

Alwall, J. 2005. Quark distributions and charged Higgs boson production. Studies of proton structure and new physics. Acta Universitatis Upsaliensis. *Digital Comprehensive Summaries of Uppsala Dissertations from the Faculty of Science and Technology* 81. 78 pp. Uppsala. ISBN 91-554-6316-9.

The Standard Model describes all elementary particles known today, but at larger energies it will have to be complemented with new particles and interactions. To be able to distinguish new physics at proton colliders such as LHC at CERN, it is essential to have an appropriate description of the colliding protons and their interactions. The study of the proton is important also in itself, to get a better understanding of the non-perturbative aspects of the strong interaction.

In paper I-IV of this thesis, a model for the non-perturbative dynamics of quarks and gluons is developed, based on quantum fluctuations in hadrons. The parton distributions of the proton are given by momentum fluctuations, with sea quark distributions generated by fluctuations into baryon-meson pairs. This model can reproduce proton structure function data, as well as measured asymmetries between up and down valence quark distributions and between the anti-up and anti-down sea. It provides an intrinsic charm quark component as indicated by data. It also predicts an asymmetry in the strange sea of the proton, which can explain the NuTeV anomaly first attributed to new physics beyond the Standard Model.

Charged Higgs bosons are predicted by several theories for new physics, including Supersymmetry. At proton colliders, the predicted dominant production mechanism is in association with top and bottom quarks. In paper V-VII, different contributions to this production are studied, and an algorithm is developed for combining the two dominant processes $gb \rightarrow tH^\pm$ and $gg \rightarrow tbH^\pm$. The algorithm gives a smooth transition from small to large transverse momenta of the b -quark, which is important when the b -quark is observed. It also gives arguments for the choice of factorisation scale in the process.

Keywords: quark densities, parton distributions, proton structure, strange quark, charm quark, charged Higgs boson, supersymmetry, NuTeV, LHC, parton showers, matrix element, elementary particle physics

Johan Alwall, Department of Radiation Sciences, Box 535, Uppsala University, SE-75121 Uppsala, Sweden

© Johan Alwall 2005

ISSN 1651-6214

ISBN 91-554-6316-9

urn:nbn:se:uu:diva-5901 (<http://urn.kb.se/resolve?urn=urn:nbn:se:uu:diva-5901>)

To my family

List of Papers

This thesis is based on the following papers, which are referred to in the text by their Roman numerals.

- I J. Alwall and G. Ingelman
“Interpretation of electron-proton scattering at low Q^2 ”
Phys. Lett. B **596** (2004) 77-83, [hep-ph/0402248](#).
- II J. Alwall and G. Ingelman
“Strange quark asymmetry in the nucleon and the NuTeV anomaly”
Phys. Rev. D **70** (2004) 111505(R), [hep-ph/0407364](#).
- III J. Alwall and G. Ingelman
“Quark asymmetries in the proton from a model for parton densities”
Phys. Rev. D **71** (2005) 094015, [hep-ph/0503099](#).
- IV J. Alwall
“Quark asymmetries and intrinsic charm in nucleons”
TSL/ISV-2005-0294 (2005), [hep-ph/0508126](#).
Extended version of “Quark asymmetries in nucleons” in the proc. of XIII International Workshop on Deep Inelastic Scattering, Madison, Wisconsin, 27 April-1 May 2005
- V J. Alwall, C. Biscarat, S. Moretti, J. Rathsman and A. Sopczak
“The $p\bar{p} \rightarrow tbH^\pm$ process at the Tevatron in HERWIG and PYTHIA simulations”
Eur. Phys. J. C **39 S1** (2004) 37-39, [hep-ph/0312301](#).
- VI J. Alwall and J. Rathsman
“Improved description of charged Higgs boson production at hadron colliders”
JHEP **12** (2004) 050, [hep-ph/0409094](#).
- VII J. Alwall
“MATCHIG: A program for matching charged Higgs boson production at hadron colliders”
TSL/ISV-2005-0290 (2005), [hep-ph/0503124](#).

Reprints were made with permission from the publishers.

Contents

| | | |
|-------|---|----|
| 1 | Introduction | 1 |
| 2 | The Standard Model - and beyond | 3 |
| 2.1 | The Standard Model | 3 |
| 2.1.1 | Gauge groups of the Standard Model | 4 |
| 2.1.2 | Abelian and non-Abelian gauge theories | 4 |
| 2.1.3 | The Higgs mechanism | 7 |
| 2.1.4 | Fields of the Standard Model | 10 |
| 2.2 | Problems with the Standard Model | 15 |
| 2.3 | Possible solutions - Extending the Standard Model | 17 |
| 2.3.1 | Supersymmetry | 18 |
| 2.3.2 | General two-Higgs-doublet models | 22 |
| 3 | QCD and parton density functions | 25 |
| 3.1 | Perturbative and non-perturbative QCD | 25 |
| 3.1.1 | Running of couplings and asymptotic freedom | 27 |
| 3.2 | Parton density functions | 30 |
| 3.2.1 | Deep inelastic scattering | 31 |
| 3.2.2 | QCD corrections to parton densities | 34 |
| 3.2.3 | The DGLAP equations | 36 |
| 3.2.4 | Parton showers | 40 |
| 3.2.5 | The starting distributions | 41 |
| 3.3 | Non-perturbative processes | 43 |
| 3.3.1 | Hadronisation | 44 |
| 3.3.2 | Parameterisations of total cross-sections | 44 |
| 3.3.3 | The hadronic photon | 47 |
| 3.4 | QCD and partons in the search for new physics | 48 |
| 3.4.1 | The NuTeV anomaly | 49 |
| 3.4.2 | QCD and new physics at the LHC | 51 |
| 4 | Summary of papers | 57 |
| 5 | Conclusions and outlook | 59 |
| 6 | Summary in Swedish – Populärvetenskaplig sammanfattning | 61 |
| | Acknowledgements | 67 |
| | Bibliography | 69 |

1. Introduction

The mission of the particle physicist is to try to understand the world at its most fundamental level, to find the smallest building-blocks of matter and how they interact. During the last century, this work has been an enormous success, culminating in the development and precision measurements of the Standard Model of particle physics.

Although the Standard Model has so far passed all experimental precision tests without any large deviations, it has inherent theoretical problems which makes it unsuitable as a final theory of the world at larger energy scales. We therefore expect that new physics, *i.e.* new particles and/or interactions, should be discovered at higher energies than those probed by present experiments. These energy scales will start being probed by the proton-proton collider LHC at CERN, which will begin operating in 2007. The signatures for new physics are expected to be difficult to distinguish from the background of Standard Model particle production, which means that in order to be able to recognise new physics when we see it, we need a very precise understanding of the colliding protons and their interactions.

The structure of the proton has been a field of continuous research since the discovery in the sixties that protons are not elementary particles. Experiments at the Stanford Linear Accelerator Center in California, where high-energy electrons were shot on a hydrogen target, showed that the proton is composed of smaller components which can be well approximated by point-like, free particles. Those particles were called partons, and were later identified with the quarks introduced by Gell-Mann and Zweig a few years before. Quarks are particles with electric charges in units of thirds of the electron charge, which had been introduced as a means to organise the multitude of strongly interacting particles, so-called hadrons, that had been discovered during the 50's. The quarks seem to exist only inside hadrons, either in triplets, constituting a baryon (for example a proton or a neutron) or paired with an anti-quark, giving a meson such as the pion. During the seventies, a theory of the interactions between quarks was developed, in which quarks are attributed a "strong charge", called a colour charge because it takes three charges to make a neutral object. This theory was called quantum chromodynamics (QCD). In 1973, Gross, Wilzcek and Politzer could show that this theory had the astonishing property of "asymptotic freedom", meaning that the harder a quark gets hit,

the weaker is the coupling of the quark to the other constituents of the hadron. This property allows calculations of hard interactions to be performed using perturbation theory, the standard method of quantum field theory.

In the opposite limit, when the momentum transfer is small, perturbative calculations are not possible. On the border between perturbative and non-perturbative QCD we find the parton density functions, describing the distributions of quarks and gluons in hadrons. The dependence of the parton densities on the hardness of the interaction can be calculated perturbatively. It is described by the so-called DGLAP evolution equations, but these only apply down to a lowest value of the momentum transfer. There, the distributions are given by non-perturbative properties of the hadron. These starting distributions are usually simply parameterized using suitable functions. In the research presented here, we have used an alternative approach to this problem: the construction of physically motivated models (papers I-IV). With the model presented in papers II-IV, which reproduces important experimental data, we get predictions for aspects of the parton density functions which are not yet well measured, and which might have impact on the search for new physics.

One very popular theory for new physics is supersymmetry, which predicts a large number of new particles. One of these particles, which also appears in other theories for new physics, is the charged Higgs boson. In paper V, we have made a comparison between two descriptions of would-be charged Higgs boson production at the Tevatron at Fermilab near Chicago, one more precise calculation and one simpler, approximate description.

One of the QCD-related effects which are important in the production of new heavy particles is parton showers, the emissions of extra quarks and gluons in an interaction. These emissions are approximately described by the DGLAP evolution equations, but to get a better description they need to be complemented by more precise calculations. If these descriptions are naively combined, it gives rise to double-counting of some emissions. In paper VI we develop an algorithm for combining the two descriptions in the case of production of charged Higgs bosons, without double-counting. We have also implemented the algorithm as an event generator program (paper VII).

The thesis is organised as follows: Chapter 2 is an overview of the Standard Model of particle physics. The theoretical problems of the theory are discussed, and some ideas on how to solve these problems are presented, in particular supersymmetry and theories with extra Higgs bosons. Chapter 3 gives an introduction to QCD and parton densities, including the DGLAP equation and the role of partons in the search for new physics. Chapter 4 is a summary of the papers included in the thesis, and Chapter 5 gives concluding remarks and outlook. Chapter 6 is a popularised summary in Swedish of the thesis.

2. The Standard Model - and beyond

The Standard Model is the theoretical framework of all particle physics known today. It is a very successful theory, which has been able to describe all elementary particles observed so far, as well as the three known forces relevant at particle physics scales and energies: the electromagnetic, strong and weak interactions. However, the theory has inherent theoretical problems, mainly connected to the electroweak symmetry breaking. To solve these, the Standard Model must be extended with new interactions and particles yet unknown. In this chapter I give an introduction to the Standard Model. I also discuss some of the ideas for extensions, focusing on those most relevant to my research.

For the interested reader who wants a more thorough technical introduction to the Standard Model and spontaneous symmetry breaking, I recommend *e.g.* [1], [2] or [3].

2.1 The Standard Model

The Standard Model is a local gauge theory. This means that the Lagrangian of the theory displays a local symmetry, *i.e.* the fields of the theory can be changed independently *at every space-time point* x without changing the form of the Lagrangian. Since the Lagrangian contains all information about the equations of motion of the fields, this implies that no experimental observables will change when we make such a transformation. How this transformation can be done is decided by the symmetry group. Symmetries in general, and gauge symmetries in particular, are of fundamental importance in elementary particle physics, and have far-reaching consequences: They relate different parameters of the model to each other, such as the couplings of fermions to gauge bosons. They also simplify calculations by allowing a choice of formalism depending on the problem at hand. And above all they stabilise the theory in such a way that it becomes renormalisable, which is a great advantage, since the theory otherwise is infinitely divergent.

Gauge theories originated with the electromagnetic theory of Maxwell. The electromagnetic theory is an Abelian (commuting) gauge theory, as was first worked out by Weyl [4], in contrast to the non-Abelian *Yang-Mills theories* [5]. As we will see, both kinds are present in the Standard Model.

2.1.1 Gauge groups of the Standard Model

The gauge groups of the Standard Model of electroweak interactions are $SU(3)_c \times SU(2)_L \times U(1)_Y$, where the $SU(3)_c$ group is the quantum chromodynamics (QCD) symmetry group of the strong interaction, the $SU(2)_L$ group is the isospin symmetry group of the weak interaction and $U(1)_Y$ is the group of weak hypercharge. The $SU(3)_c$ group and its implications will be discussed in chapter 3. Its presence does not affect the electroweak theory discussed here, and I will therefore omit all references to $SU(3)_c$ in this chapter.

The idea of unifying the electromagnetic and the weak interactions using the combined group $SU(2)_L \times U(1)_Y$, where the $SU(2)$ symmetry must be broken, was first put forward by Glashow in 1961 [6], but it was Weinberg (1967) [7] and, independently, Salam (1968) [8], who included the Higgs mechanism to make the theory renormalisable. The proof that it was indeed renormalisable was achieved by 't Hooft [9], who worked out a general proof for the renormalisability of gauge theories, with and without spontaneous symmetry breaking. In the Weinberg-Salam model, the $SU(2)_L \times U(1)_Y$ symmetry is broken down to the electromagnetic $U(1)_Q$ group through the *Higgs phenomenon*, giving rise to the massive W^\pm and Z bosons as well as the masses of fermions via Yukawa interactions, in contrast to the massless bosons and fermions of the theory before symmetry breaking. In order to understand why and how this comes about, I first give an introduction to local gauge theories, then I discuss the Higgs phenomenon before returning to the particle content and structure of the Standard Model.

2.1.2 Abelian and non-Abelian gauge theories¹

As described above, a local gauge symmetry means that the fields of the theory can be changed at any space-time point without changing the physics. As we will see, this demands the introduction of interactions into the theory, mediated by massless vector bosons (in the electromagnetic case these are the photons). The electromagnetic interaction is an Abelian *local* $U(1)$ *symmetry*, which means that we can transform the electron field ψ through

$$\psi(x) \longrightarrow \psi'(x) = e^{-i\alpha(x)}\psi(x) \quad (2.1)$$

where $\alpha(x)$ is a real function of x .

The Dirac Lagrangian of a non-interacting electron is

$$\mathcal{L}_0 = \bar{\psi}(x)(i\gamma^\mu\partial_\mu - m)\psi(x) \quad (2.2)$$

¹In this section I follow the sign conventions of [3].

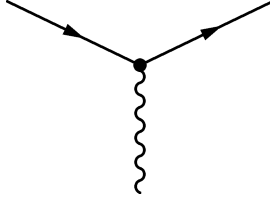


Figure 2.1: The interaction vertex between the fermion (represented by the plain line) and the vector boson (the wiggly line) in the Abelian gauge theory.

In order to make this Lagrangian invariant under the $U(1)$ transformation, we must introduce a *gauge vector field* $A_\mu(x)$ into the theory:

$$\mathcal{L} = \bar{\psi}(x)(i\gamma^\mu(\partial_\mu + ieA_\mu(x)) - m)\psi(x) = \bar{\psi}(x)(i\gamma^\mu D_\mu - m)\psi(x) \quad (2.3)$$

where we have introduced the covariant derivative $D_\mu = \partial_\mu + ieA_\mu$. The introduction of the gauge field also introduces an interaction between ψ and A_μ with a coupling e and a vertex as shown in fig. 2.1.

The gauge field must then transform as

$$A_\mu(x) \longrightarrow A'_\mu(x) = A_\mu(x) + \frac{1}{e}\partial_\mu\alpha(x) \quad (2.4)$$

The gauge vector field A_μ is identified with the electromagnetic four-potential, and has the gauge-invariant kinetic energy term

$$\mathcal{L}_V = -\frac{1}{4}F_{\mu\nu}F^{\mu\nu} \quad (2.5)$$

where

$$F_{\mu\nu} = \partial_\mu A_\nu - \partial_\nu A_\mu \quad (2.6)$$

is the *field strength*. This is just the kinetic energy Lagrangian Maxwell proposed for the electromagnetic field.

The simplest example of a *non-Abelian*, *i.e.* non-commuting, gauge symmetry is invariance under local $SU(2)$ transformations. Under a local $SU(2)$

transformation, a doublet field $\Psi(x) = \begin{pmatrix} \psi_1(x) \\ \psi_2(x) \end{pmatrix}$ transforms as

$$\Psi(x) \longrightarrow \Psi'(x) = \exp\left\{\frac{-i\tau_j\theta^j(x)}{2}\right\}\Psi(x) \quad (2.7)$$

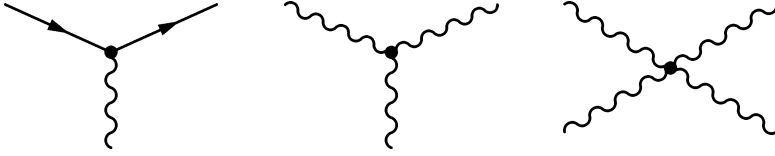


Figure 2.2: The interaction vertices of the non-Abelian theory: In addition to the fermion-vector boson vertex, there are also 3- and 4-vector boson vertices.

where $\theta^{1,2,3}(x)$ are real functions parameterising the $SU(2)$ transformation, and $\tau_{1,2,3}$ are the Pauli matrices. They are traceless Hermitian 2×2 matrices satisfying the commutation relations

$$[\tau_i, \tau_j] \equiv \tau_i \tau_j - \tau_j \tau_i = 2i \epsilon_{ijk} \tau_k, \quad i, j, k = 1, 2, 3 \quad (2.8)$$

where ϵ_{ijk} is the totally antisymmetric tensor. The term “non-Abelian” refers to the property that the generators of the group, in this case $\tau_{1,2,3}/2$, have non-zero commutation relations with each other.

Since we want to make the Lagrangian of the Dirac field invariant under a local $SU(2)$ transformation, we once again need to introduce gauge fields. In this case there must be three of them, $\{A_\mu^i\}$, $i = 1, 2, 3$, one for each generator τ_i . The covariant derivative becomes

$$D_\mu = \partial_\mu - ig \frac{\tau_i A_\mu^i}{2} \quad (2.9)$$

where A_μ^i now has the transformation properties (for infinitesimal transformations)

$$A_\mu^{i'} = A_\mu^i + \epsilon^{ijk} \theta^j A_\mu^k - \frac{1}{g} \partial_\mu \theta^i \quad (2.10)$$

In the non-Abelian $SU(2)$ case, the invariant kinetic energy term is given by

$$\mathcal{L}_V = -\frac{1}{4} F_{\mu\nu}^i F^{i\mu\nu} \quad (2.11)$$

where the field strength is now

$$F_{\mu\nu}^i = \partial_\mu A_\nu^i - \partial_\nu A_\mu^i + g \epsilon^{ijk} A_\mu^j A_\nu^k \quad (2.12)$$

Note that the last term in eq. (2.12) constitutes an interaction between two different gauge fields. Looking closer at eq. (2.11), we see that we get interaction vertices with three and four gauge bosons, as depicted in fig. 2.2. In contrast to the Abelian electromagnetic case, the gauge bosons A_μ^i interact with each other in non-Abelian gauge theories.

2.1.3 The Higgs mechanism

In a gauge theory, the gauge fields must be massless. The reason is that a mass term of the type $\frac{1}{2}M^2 A_\mu A^\mu$ would break the gauge invariance of the Lagrangian, since the transformation (2.4) would introduce new terms dependent on $\alpha(x)$ in the Lagrangian. However, in the real world, the interaction vector bosons of the weak interaction are very heavy (their masses are 85 – 95 proton masses, *i.e.* heavier than a copper atom). This means that the gauge symmetry must be broken in nature. The simplest way to accomplish this would be to simply introduce mass terms for the vector bosons in the Lagrangian, thereby explicitly breaking the symmetry. This path was attempted by Glashow [6]. Unfortunately, it turned out that such a theory is not renormalisable. The solution, first conceived for the case of a global symmetry by Nambu [10] and Goldstone [11], is to keep the symmetry in the Lagrangian but have a *symmetry-breaking vacuum*. This approach is called *spontaneous symmetry breaking*. The simplest method to accomplish it for a local gauge symmetry is through the *Higgs mechanism* [12]. In order to explain the Higgs mechanism, spontaneous breaking of an Abelian ($U(1)$) gauge theory will be taken as an example, which is then applied to the non-Abelian situation in the Standard Model.

Abelian symmetry breaking

Starting out with the Abelian $U(1)$ case, we want to construct a theory in which a vacuum breaks the symmetry and gives mass to the gauge boson. In order to accomplish this, we introduce a complex scalar field ϕ , which transforms under the $U(1)$ transformation according to eq. (2.1). It couples to the gauge boson through a $U(1)$ -invariant Lagrangian

$$\mathcal{L}_\phi = |(\partial_\mu - igA_\mu)\phi|^2 - V(|\phi|^2) \quad (2.13)$$

with the potential

$$V(|\phi|^2) = \mu^2 \phi^\dagger \phi + \lambda (\phi^\dagger \phi)^2 \quad (2.14)$$

If we let μ^2 be negative and λ positive, the scalar field potential gets a shape

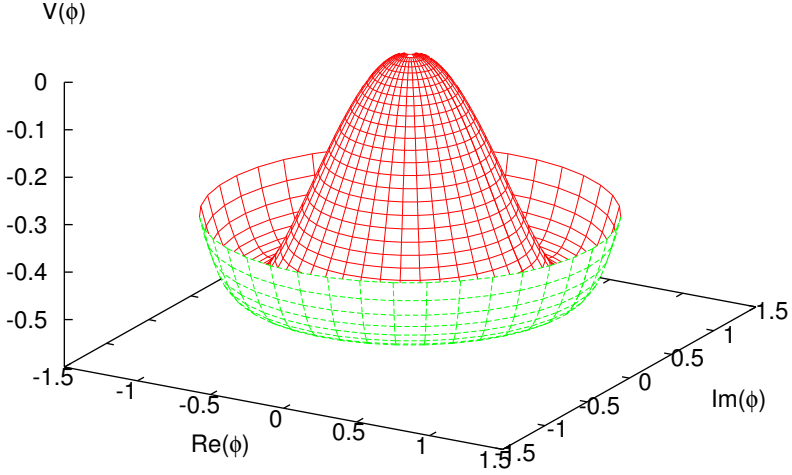


Figure 2.3: The “Mexican hat” Higgs potential with $\mu^2 = -1, \lambda = 1/2$ giving $v = \sqrt{2}$. Note that the minimum of the potential is rotationally invariant, and the symmetry is broken when a specific direction is chosen for the vacuum expectation value.

like a Mexican hat, shown in fig. 2.3. This potential has its minimum when

$$|\phi| = \frac{v}{\sqrt{2}}, \quad v = \sqrt{-\frac{\mu^2}{\lambda}} \quad (2.15)$$

The vacuum expectation value (vev) of a field is at the minimum of the potential. This means that the field ϕ gets a non-zero vev $|\langle\phi\rangle_0| = \frac{v}{\sqrt{2}}$. This minimum is symmetric with respect to rotations in the complex plane. The symmetry breaking that we seek comes about when a certain direction is chosen for the vev, *e.g.* along the positive real axis.

If we now make an expansion of the field around this vacuum:

$$\phi = \frac{1}{\sqrt{2}}(v + \phi_1 + i\phi_2) \quad (2.16)$$

we get for the kinetic part of the Lagrangian

$$\begin{aligned} \mathcal{L}_\phi^{\text{kin}} &= |D_\mu\phi|^2 = \frac{1}{2}|(\partial_\mu - igA_\mu)(v + \phi_1 + i\phi_2)|^2 = \\ &= \frac{1}{2}|D_\mu\phi_1|^2 + \frac{1}{2}|D_\mu\phi_2|^2 + gA^\mu(\phi_2\partial_\mu\phi_1 - \phi_1\partial_\mu\phi_2) + \\ &\quad + g^2v\phi_1A^\mu A_\mu - gvA^\mu\partial_\mu\phi_2 + \frac{1}{2}g^2v^2A^\mu A_\mu \end{aligned} \quad (2.17)$$

The last term is just a mass term for the gauge field, corresponding to a mass $m_A = gv$. However, this mass term has a prize: A massive vector field has three degrees of freedom, two transverse polarisation directions and one longitudinal, while a massless field has only the two transverse polarisation directions. Therefore it would appear that we have introduced one extra degree of freedom by just making the change of variables (2.16). Fortunately, this is not the case, as can be shown by making a special choice of gauge (the *unitary gauge*), in which the scalar field is purely real; that this can be done is easily seen from eq. (2.1). Using this gauge, the imaginary component ϕ_2 is transformed away. It is instead absorbed into the vector field, effectively becoming the longitudinal polarisation component of the vector field. The remaining scalar field then gets a mass $m_{\phi_1} = \sqrt{-2\mu^2}$. This remaining field is the *Higgs particle*.

$SU(2)$ symmetry breaking

In the Standard Model, the broken symmetry is the non-Abelian $SU(2)_L$ symmetry. The mechanism for this case is very similar to the Abelian case above. Again, we introduce a scalar field, but this time in the form of an $SU(2)$ doublet $\Phi = \begin{pmatrix} \phi^+ \\ \phi^0 \end{pmatrix}$. It transforms according to eq. (2.7) and couples to the vector fields through the Lagrangian

$$\mathcal{L}_\Phi = (D_\mu \Phi)^\dagger (D_\mu \Phi) - V(\Phi) \quad (2.18)$$

where

$$D_\mu = \partial_\mu - ig \frac{\tau_i A_\mu^i}{2} \quad \text{and} \quad V(\Phi) = \mu^2 (\Phi^\dagger \Phi) + \lambda (\Phi^\dagger \Phi)^2 \quad (2.19)$$

Assuming $\mu^2 < 0$ we again get a minimum of the potential at $\Phi^\dagger \Phi = -\frac{1}{2} \frac{\mu^2}{\lambda}$, giving a vacuum expectation value for the field

$$\langle \Phi^\dagger \Phi \rangle_0 = \frac{v^2}{2}, \quad v = \sqrt{-\frac{\mu^2}{\lambda}} \quad (2.20)$$

Just as before, the gauge symmetry is spontaneously broken when a certain direction for the vev is chosen. In the Standard Model, the lower component of the Higgs doublet is electrically neutral and the upper is charged. We want the vacuum to be electrically neutral, and therefore choose to give the neutral component of the doublet a non-vanishing vev, keeping the expectation value

| Generation | I | II | III |
|------------|---------------------------|-------------------------------|---------------------------------|
| Quarks | up (u) | charm (c) | top (t) |
| | down (d) | strange (s) | bottom (b) |
| Leptons | e -neutrino (ν_e) | μ -neutrino (ν_μ) | τ -neutrino (ν_τ) |
| | electron (e) | muon (μ) | tauon (τ) |

Table 2.1: The three generations of quarks and leptons in the Standard Model.

of the charged component zero:

$$\langle \Phi \rangle_0 = \frac{1}{\sqrt{2}} \begin{pmatrix} 0 \\ v \end{pmatrix} \quad (2.21)$$

We can once again make an expansion of the fields around this vacuum, and once again we get a mass term for the gauge vector fields from the kinetic part of the Lagrangian, $(D_\mu \Phi)^\dagger (D_\mu \Phi)$, but in this case the masses of the vector fields become $m = gv/2$. Note that there are now three degrees of freedom with zero vev, the real and imaginary upper component and the imaginary lower component. Using the unitary gauge, we can show that these three fields are absorbed by the three vector bosons of the $SU(2)$ gauge symmetry, to become their longitudinal polarisation components. Also in this case we are left with one physical scalar Higgs particle.

2.1.4 Fields of the Standard Model

In the Standard Model, there are two kinds of matter fields: leptons and quarks. While the leptons are only affected by the electroweak interaction, the quarks are effected by both the electroweak and strong interactions. The leptons and quarks can be arranged in three generations of field doublets, as shown in table 2.1. The different kinds of quarks, u , d , s , c , b and t , and leptons, e , μ , τ and their neutrinos, are called *flavours*. For the treatment of electroweak symmetry breaking and the Higgs mechanism, the presence of more than one generation is not important, since the structure of the weak interactions of the second and third generations is identical to that of the first. I will therefore only take into account the first generation in the following. There are however several interesting phenomena associated with the presence of several generations, such as mixing of states and CP -violation. For the interested reader, I recommend the presentation in [3].

In the absence of electroweak symmetry breaking, all the matter fields (fermions) and gauge bosons of the Standard Model are massless. The matter

| Field | Spin | Mass | Y | $SU(2)_L$ | $SU(3)$ | # of states |
|---|---------------|------|----------------|-----------|----------|-------------|
| $Q_L = \begin{pmatrix} u_L \\ d_L \end{pmatrix}$ | $\frac{1}{2}$ | 0 | $+\frac{1}{3}$ | 2 | 3 | 6 |
| u_R | $\frac{1}{2}$ | 0 | $+\frac{4}{3}$ | 1 | 3 | 3 |
| d_R | $\frac{1}{2}$ | 0 | $-\frac{2}{3}$ | 1 | 3 | 3 |
| $L_L = \begin{pmatrix} \nu_{eL} \\ e_L \end{pmatrix}$ | $\frac{1}{2}$ | 0 | -1 | 2 | 1 | 2 |
| e_R | $\frac{1}{2}$ | 0 | -2 | 1 | 1 | 1 |

\Downarrow *The Higgs mechanism*

| Field | Spin | Mass | Q | $SU(3)$ | # of states |
|------------|---------------|-------|----------------|----------|-------------|
| u | $\frac{1}{2}$ | m_u | $+\frac{2}{3}$ | 3 | 6 |
| d | $\frac{1}{2}$ | m_d | $-\frac{1}{3}$ | 3 | 6 |
| e | $\frac{1}{2}$ | m_e | -1 | 1 | 2 |
| ν_{eL} | $\frac{1}{2}$ | 0 | 0 | 1 | 1 |

Table 2.2: Matter content of the Standard model before and after spontaneous symmetry breaking through the Higgs mechanism. Y is the hypercharge and Q is the electric charge. The last column shows the number of states in each field. Note that all particles have antiparticles, which are not indicated.

fields are organised such that the left-handed fields are ordered in $SU(2)$ doublets, while the right-handed fields are $SU(2)$ singlets. Since Dirac mass terms couple right-handed and left-handed fields, such terms would break $SU(2)$ invariance. Therefore it is only after the spontaneous symmetry breaking that the matter fields get mass, by means of so-called Yukawa couplings to the Higgs field, as will be shown below. The field content of the theory, before and after symmetry breaking, is shown in the tables 2.2 and 2.3. Note that there is no right-handed neutrino in this minimal version of the Standard Model, although it is possible to include non-interacting (sterile) right-handed neutrinos in the model in order to allow for neutrino masses of Dirac type. Also note that in table 2.2, only the first generation particles are present, but the structure is the same for the second and third generation.

The Lagrangian of the Standard Model gives the interactions of the fields

| Field | Spin | Mass | Y | $SU(2)$ | # of states |
|---|------|------------------|-----|----------|-------------|
| $A_\mu^{1,2,3}$ | 1 | 0 | 0 | 3 | 6 |
| B_μ | 1 | 0 | 0 | 1 | 2 |
| $\Phi = \begin{pmatrix} \phi^+ \\ \phi^0 \end{pmatrix}$ | 0 | <i>imaginary</i> | +1 | 2 | 4 |

⇓ *The Higgs mechanism*

| Field | Spin | Mass | Q | # of states |
|-------------|------|-------|---------|-------------|
| W_μ^\pm | 1 | m_W | ± 1 | 6 |
| Z_μ | 1 | m_Z | 0 | 3 |
| A_μ | 1 | 0 | 0 | 2 |
| H | 0 | m_h | 0 | 1 |

Table 2.3: Gauge and Higgs bosons of the unbroken $SU(2)_L \times U(1)_Y$ theory, and after spontaneous symmetry breaking.

before symmetry breaking, and can be decomposed into the following parts:

$$\mathcal{L} = \mathcal{L}_V + \mathcal{L}_f + \mathcal{L}_h + \mathcal{L}_Y \quad (2.22)$$

We first have

$$\mathcal{L}_V = -\frac{1}{4}F_{\mu\nu}^i F^{i\mu\nu} - \frac{1}{4}G_{\mu\nu} G^{\mu\nu} \quad (2.23)$$

which is the kinetic energy of the vector gauge fields, with $F_{\mu\nu}^i = \partial_\mu A_\nu^i - \partial_\nu A_\mu^i + g\epsilon^{ijk} A_\mu^j A_\nu^k$, $i, j, k = 1, 2, 3$ and $G_{\mu\nu} = \partial_\mu B_\nu - \partial_\nu B_\mu$. Here $A_\mu^{1,2,3}$ are the three vector fields of the $SU(2)_L$ gauge symmetry and B_μ is the vector field of the hypercharge $U(1)_Y$ symmetry. As we will see, the hypercharge is related to the electric charge Q after symmetry breaking, and the vector field B_μ to the electromagnetic gauge field A_μ .

$$\begin{aligned} \mathcal{L}_f = & \bar{L}_L i\gamma^\mu D_\mu^L L_L + \bar{e}_R i\gamma^\mu D_\mu^e e_R + \bar{Q}_L i\gamma^\mu D_\mu^Q Q_L + \\ & \bar{u}_R i\gamma^\mu D_\mu^u u_R + \bar{d}_R i\gamma^\mu D_\mu^d d_R \end{aligned} \quad (2.24)$$

is the fermionic kinetic energy Lagrangian, where

$$D_\mu^{L,Q} = \left(\partial_\mu - ig \frac{\tau_i}{2} A_\mu^i - ig' \frac{Y}{2} B_\mu \right) \quad (2.25)$$

are the covariant derivatives for the doublet fields L_L and Q_L and

$$D_\mu^{e,u,d} = \left(\partial_\mu - ig' \frac{Y}{2} B_\mu \right) \quad (2.26)$$

are for the singlet fields e_R, u_R, d_R . As before, $\tau_i/2$ are the $SU(2)$ generators, which only act on the $SU(2)_L$ doublet fields L_L and Q_L . Note that we have two couplings for the two gauge groups; g is the coupling of the doublet fields to the $SU(2)$ gauge fields, and g' is the coupling to the hypercharge gauge field.

$$\mathcal{L}_H = (D_\mu^H \Phi)^\dagger (D^{H\mu} \Phi) - V(\Phi) \quad (2.27)$$

is the Higgs boson kinetic and potential Lagrangian. The Higgs doublet has hypercharge $Y = +1$ and has the covariant derivative

$$D_\mu^H = \left(\partial_\mu - ig \frac{\tau_i}{2} A_\mu^i + \frac{ig'}{2} B_\mu \right) \quad (2.28)$$

while $V(\Phi) = \mu^2 \Phi^\dagger \Phi + \lambda (\Phi^\dagger \Phi)^2$ is the Higgs potential which we recognise from section 2.1.3.

Finally,

$$\mathcal{L}_Y = f^{(e)} (\bar{L}_L \Phi) e_R + f^{(u)} (\bar{Q}_L \tilde{\Phi}) u_R + f^{(d)} (\bar{Q}_L \Phi) d_R + \text{h.c.} \quad (2.29)$$

are the Yukawa couplings, giving the interactions between the fermions and the Higgs scalars (h.c. stands for ‘‘hermitian conjugate’’). $f^{(a)}$, $a = e, u, d$ are called Yukawa coupling constants and $\tilde{\Phi} = i\tau_2 \Phi^*$ has hypercharge $Y = -1$.

This Lagrangian is invariant under $SU(2)_L$ and $U(1)_Y$ transformations. Note that there are no mass terms, neither for the vector bosons nor for the fermions, as discussed above.

If we now let the Higgs potential mass term μ^2 be negative, the Higgs phenomenon occurs, giving the neutral component of the Higgs doublet a vacuum expectation value as described in sec. 2.1.3. Three of the scalar degrees of freedom are absorbed by three massive vector fields, and we are left with one physical Higgs particle H . However, in this scenario, also the fermions gain mass in the symmetry breaking. This is due to the Yukawa terms in eq. (2.29), which couple left-handed and right-handed fields and thereby create mass

terms for the Dirac fields e, u, d . Indeed, by expanding around the vacuum expectation value we get

$$\begin{aligned} \mathcal{L}_Y = & \frac{H(x)}{\sqrt{2}} [f^{(e)} \bar{e}_L e_R + f^{(u)} \bar{u}_L u_R + f^{(d)} \bar{d}_L d_R] + \\ & + \frac{v}{\sqrt{2}} [f^{(e)} \bar{e}_L e_R + f^{(u)} \bar{u}_L u_R + f^{(d)} \bar{d}_L d_R] + \text{h.c.} \end{aligned} \quad (2.30)$$

From this equation we can read off the masses of the particles: $m_e = f^{(e)} v / \sqrt{2}$, $m_u = f^{(u)} v / \sqrt{2}$, $m_d = f^{(d)} v / \sqrt{2}$. Note that the values for these masses are not predicted by the theory, since the Yukawa couplings are arbitrary.

As the Higgs mechanism breaks the $SU(2)_L$ symmetry, giving all three $SU(2)$ vector fields A_μ^i mass, we should be left with the $U(1)_Y$ symmetry. However, in the Lagrangian (2.27), the Higgs field couples also to the hypercharge gauge field B_μ , so we get a mass term for this field as well. This apparent contradiction is solved by observing that the remaining symmetry is not the hypercharge $U(1)_Y$, but the electromagnetic $U(1)_Q$, where

$$Q = T_3 + \frac{Y}{2} \implies Y = 2(Q - T_3) \quad (2.31)$$

Here T_3 is the weak isospin along the third component (0 for $SU(2)$ singlets, $+\frac{1}{2}$ for the upper component of an $SU(2)$ doublet and $-\frac{1}{2}$ for the lower component of an $SU(2)$ doublet). The charge of the different fields after symmetry breaking is shown in the lower part of table 2.2. This also means that the massless (electromagnetic) gauge field A_μ is a linear combination of the neutral weak gauge field A_μ^3 and the hypercharge gauge field B_μ . The same is true for the neutral massive vector field Z_μ , while the W_μ^\pm are defined by A_μ^1 and A_μ^2 :

$$A_\mu = \frac{g' A_\mu^3 + g B_\mu}{\sqrt{g^2 + g'^2}} = \sin \theta_W A_\mu^3 + \cos \theta_W B_\mu \quad (2.32a)$$

$$Z_\mu = \frac{g A_\mu^3 - g' B_\mu}{\sqrt{g^2 + g'^2}} = \cos \theta_W A_\mu^3 - \sin \theta_W B_\mu \quad (2.32b)$$

$$W_\mu^+ = \frac{1}{\sqrt{2}} (A_\mu^1 - i A_\mu^2) \quad (2.32c)$$

$$W_\mu^- = \frac{1}{\sqrt{2}} (A_\mu^1 + i A_\mu^2) \quad (2.32d)$$

The quantity θ_W , defined by $\tan \theta_W = g' / g$, determines the mixing be-

tween the weak and electromagnetic forces. It is called the *Weinberg angle*, and is usually given as $\sin^2 \theta_W$, which is measured to quite high precision [13]:

$$\sin^2 \theta_W = 0.22272 \pm 0.00036 \quad (2.33)$$

The electromagnetic coupling constant (*i.e.* the electric charge of the electron) is then $e = g \sin \theta_W = g' \cos \theta_W$.

In the same way as in sec. 2.1.3, we can find expressions for the masses of the massive vector bosons, taking into account the mixing (2.32). These expressions, and the experimental values for the masses [14], are

$$\begin{aligned} m_W &= \frac{1}{2}vg = 80.425 \pm 0.038 \text{ GeV} \\ m_Z &= \frac{m_W}{\cos \theta_W} = 91.1876 \pm 0.0021 \text{ GeV} \end{aligned} \quad (2.34)$$

Note that in the Standard Model, the quantity

$$\rho = \frac{M_W^2}{M_Z^2 \cos^2 \theta_W} = 1 \quad (2.35)$$

at tree-level (*i.e.* taking into account only diagrams without loops). Loop corrections give $\rho = 1.0055 \pm 0.0005$, and the experimental value is 1.0054 ± 0.0010 [15].

The vacuum expectation value v for the Higgs can be calculated from the Fermi coupling constant

$$G = \frac{g^2}{4\sqrt{2}m_W^2} = \frac{1}{\sqrt{2}v^2} = 1.16637 \cdot 10^{-5} \pm 0.00001 \cdot 10^{-5} \text{ GeV}^{-2} \quad (2.36)$$

giving $v = 246 \text{ GeV}$.

Note that the theory doesn't give any prediction for the Higgs mass, since the value of μ^2 cannot be deduced from the masses and couplings of the other particles.

2.2 Problems with the Standard Model

The theory described above is extremely successful. It predicted the mass and properties of the W and Z bosons before they were discovered at the SPS collider at CERN in 1983 [16], as well as (through loop corrections) the mass and couplings of the top quark [17] before its discovery at the Tevatron in

1995 [18]. All known elementary particles, and their properties, are accurately described in the theory (see [13] for the most recent global fit of experimental data to the Standard Model). However, there are also problems. The most conspicuous is: Where is the Higgs particle? The global fit to Standard Model parameters gives a Higgs boson mass of 98_{-26}^{+52} GeV (with 1σ uncertainties) [19]. The best-fit value 98 GeV is below the direct exclusion limit by LEP2 of 114.4 GeV (at 95% confidence level) [20], already making the Standard Model with the Higgs mechanism slightly improbable.

This is however just a small detail compared with the theoretical problems facing the theory, and which also have to do mainly with the Higgs sector. The problem is that, as higher-order (radiative) corrections to the theory are calculated, the Higgs boson mass receives very large corrections. To one-loop order these are proportional to the square of some cutoff-scale Λ (see *e.g.* [21]):

$$\delta m_H^2 = \frac{3}{8\pi^2 v^2} (4m_t^2 - 2m_W^2 - 4m_Z^2 - m_H^2) \Lambda^2 \quad (2.37)$$

The cutoff Λ can be identified with the momentum scale where new physics sets in. If the Standard Model were the definite theory of reality up to the Planck scale (where gravity starts to become important, and therefore new physics must be introduced that can combine gravity with quantum field theory), the corrections to the Higgs mass are of the order $M_{\text{Pl}} \sim 10^{19}$ GeV. However, the Higgs mass cannot be larger than ~ 800 GeV in order to conserve tree-level unitarity of the S-matrix of vector boson scattering [22]. In the Standard Model, the only solution to this problem is *fine-tuning*, *i.e.* to let the bare Higgs mass before the addition of radiative corrections perfectly balance the radiative corrections. With radiative corrections for m_H^2 of the order M_{Pl}^2 , this would imply that the bare mass-squared must be precisely tuned to better than one part in 10^{32} . This is called the *naturalness* or *hierarchy* problem. A theory is considered *natural* if the observable properties of the theory, such as masses, are stable under small variations of the fundamental parameters [23]. To preserve naturalness of the Standard Model some new physics must set in at a mass scale around 1 TeV [21]. In the next section I will discuss a few alternatives for theories of new physics which are popular today.

There are also some more “aesthetical” problems with the Standard Model. One is that the theory doesn’t give any explanation to why the constants of the model have the values they have. For example, the Yukawa couplings of the fermions to the Higgs field vary over five orders of magnitude (unless we assume that neutrino masses are Dirac-like and generated by the same mechanism – then it is at least eleven orders of magnitude!), and we have no clue as to why. Also the symmetry group itself, $SU(3)_c \times SU(2)_L \times U(1)_Y$, is composed of three distinct gauge symmetries, which may seem unaesthetical.

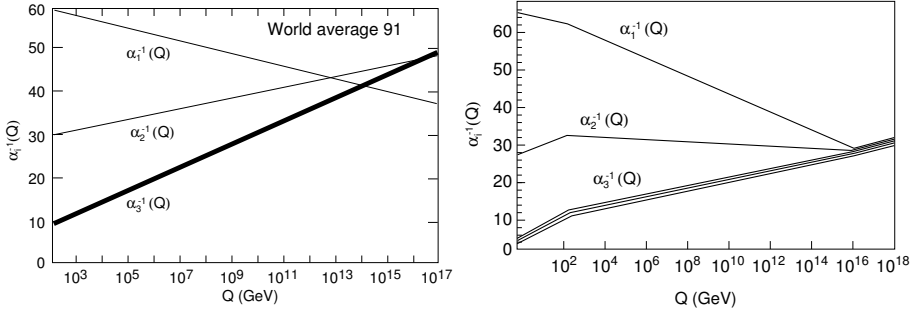


Figure 2.4: Evolution of the gauge couplings (a) in the Standard Model (b) in the MSSM with SUSY masses close to 1 TeV [25]. The plots are from [26].

There have been many attempts to explain the structure of the Standard Model by assuming that there is some larger symmetry group which is broken at some large scale, a Grand Unified Theory (GUT), as was first done by Georgi and Glashow [24]. The presence of such a unification is also suggested by the running of the gauge couplings by the renormalization group equations (which will be discussed in chapter 3, sec. 3.1.1). For a long time the couplings appeared to meet at a scale near 10^{15} GeV. Unfortunately, newer, more precise data has revealed that they don't really meet, unless there are some new fields in the mass regions between the electroweak scale and the GUT scale. This is the case with the inclusion of low-scale supersymmetry [25], see fig. 2.4.

There is one actual observational indication that the particle spectrum of the Standard Model must be extended. Cosmological observations imply that a large part of the matter density in the universe consists of non-baryonic particles moving with low speeds, so called “cold dark matter” [27]. No particle in the Standard Model meets with the demands from cosmological data, and therefore new physics must be introduced in order to explain these observations. Yet another recent problem for the Standard Model is the observation of neutrino oscillations by the SNO neutrino observatory in 2001 [28], which implies that neutrinos must have mass. However, these very interesting topics are out of scope for this thesis, and I will not elaborate on them here.

2.3 Possible solutions - Extending the Standard Model

That the Standard Model is a spontaneously broken gauge theory with the gauge group $SU(3)_c \times SU(2)_L \times U(1)_Y$ is very well supported by experimental evidence. However, since we haven't observed the Higgs boson, we still don't have any indications of how breaking of the weak $SU(2)_L$ sym-

metry is accomplished in nature. Therefore there is room for different ideas concerning this very important aspect of the theory, although any new model must conform to the precise experimental measurements, which allow only very small departures from the Standard Model predictions (*cf.* [29]). This puts strong limitations on possible models. The efforts to solve the problems of the weak symmetry breaking can be summarised in the following main groups:

- Keep the Higgs mechanism, but protect the Higgs mass from large radiative corrections by introducing some new symmetry. Along this direction we have Supersymmetry (which will be discussed below) and Little Higgs theories, in which the Higgs boson is a so-called pseudo-Goldstone boson [30].
- Get rid of the Higgs (at least as a fundamental scalar). This is accomplished in Technicolour theories, where the electroweak $SU(2)_L$ symmetry is broken dynamically (in a way similar to the chiral symmetry breaking in QCD), and the Higgs particle corresponds to a condensate of fermions [31]. There are also recent attempts to create Higgs-less theories, where boundary conditions in extra dimensions break the symmetry [32], and there is no Higgs particle at all.
- Get rid of the large mass hierarchy altogether, by approaching the Planck scale to the electroweak scale. This can be achieved by considering large extra dimensions (with radii up to 1 mm) [33]. In these models, the Planck scale is actually around 1 TeV, but gravity appears weak because it can propagate in the extra dimensions.

To this list one can also add “minimal” extensions to the Standard Model, which don’t change the structure of the model. One such example has already been mentioned, namely Dirac mass terms for the neutrinos by Yukawa couplings. Another is the inclusion of extra Higgs doublets and/or singlets, enhancing the particle spectrum in the Higgs sector. In such theories with extended Higgs sectors, the experimental limits and constraints on parameters of the theory, such as the Higgs mass, can be relaxed considerably [34].

My research has so far only involved supersymmetry and extended Higgs sectors, and in the following sections I will therefore focus on those topics.

2.3.1 Supersymmetry

Supersymmetry is interesting, not least for the attention, and acceptance, it has received in the high energy physics community. It is a theory which is “too beautiful not to be true”, and many physicists regard it as almost unthinkable that it shouldn’t be realised at some energy scale. The big problem is again: Where is it? The search for supersymmetry in experiments has been going on for more than 20 years (see *e.g.* [35]), and there has yet been no

sign of it. The last hope of low-energy supersymmetry is probably the LHC; if the LHC doesn't show any trace of superparticles, it might well be the end of supersymmetry as a solution to the problems with electroweak symmetry breaking. But we are not there yet!

In this thesis, I will not go into the details of the mathematics of supersymmetry and graded Lie algebras, since I have mainly been working with the Higgs sector of the minimal supersymmetric extension to the Standard Model. For the interested reader, the book by Weinberg [36] gives a thorough review. There are excellent books concentrating on the mathematics of supersymmetric field theory [37]. For shorter reviews on supersymmetric extensions to the Standard Model, see *e.g.* [38].

Supersymmetry was first applied to four-dimensional space-time by Wess and Zumino in 1973 [39]. It is the largest possible enhancement of the symmetries of space and time [40], and this is a reason in itself why it is so endorsed (why should space-time be less than maximally symmetric?). It corresponds to a symmetry between bosons and fermions, meaning that every fermion must have a corresponding boson and vice versa, in such a way that the number of bosonic states is equal to the number of fermionic states. This is induced by the enhanced space-time symmetry in a similar way that the Lorentz invariance imposes that every particle must have an antiparticle. The partners of fermions are denoted by an “s” (for scalar) before the name of the matter particle, such as “selectron”, “stop”, “sbottom”, and generally “sleptons” and “squarks”. The partners of bosons get the suffix “-ino”: “higgsino”, “gluino”, “wino”. The fermionic partners of the neutral electroweak gauge and Higgs bosons have mixed mass eigenstates called “neutralinos”, and in the same way we get “charginos” from the mixed charged fermionic superpartners.

These superpartners must have the same properties (couplings, masses, quantum numbers) as their particles, except of course for the spin. Therefore supersymmetry is apparently not (exactly) realised in nature, since we then should have seen a charged scalar particle with the mass and couplings of the electron, and similarly for all other particles we know. However, it is still possible that the supersymmetry is an approximate symmetry, which is broken below some mass scale above the electroweak scale, in a similar manner that electroweak symmetry is broken. The superpartners could in this case differ from the Standard Model fields, not only with respect to their spin, but also in their mass, which can then be quite large.

The introduction of superpartners solves the problem of the instability of the Higgs mass. This is due to a special property of fermions and bosons: In a Feynman diagram, a loop with a fermionic particle comes with a negative sign relative to a loop with a bosonic particle. Therefore, the quadratic divergences in the corrections to the Higgs mass due to loops of Standard Model fields will be exactly cancelled by the corresponding loops containing the superpartners,

no matter how many loops we calculate (*i.e.* at all orders in perturbation theory):

$$\delta m_H^2 \sim \frac{\alpha}{2\pi}(\Lambda^2 + m_B^2) - \frac{\alpha}{2\pi}(\Lambda^2 + m_F^2) + \text{logarithmic divergences} \quad (2.38)$$

This is quite remarkable, and is the main reason why supersymmetry has been so widely accepted. This cancellation still works when supersymmetry is broken, as long as it is done in a special manner, called *soft supersymmetry breaking* [41]. This amounts to insertion of “soft” supersymmetry breaking terms, *e.g.* mass terms for the supersymmetric partners, in the supersymmetric Lagrangian. The value of these masses (especially the top partner, *stop*, mass) then corresponds to a new cutoff-scale Λ . This means that if we are to avoid too large fine-tuning of the Higgs mass, the supersymmetric masses ought to be below or around 1 TeV, and should be observable at the LHC.

Supersymmetry also has other nice features. As mentioned above, the addition of supersymmetric partner particles with masses around 1 TeV changes the running of the couplings for the strong, weak and electromagnetic interactions in such a way that they all meet at a mass scale around 10^{16} GeV [25], which is a hint that if supersymmetry is present, then grand unification is still possible. Another nice feature occurs if a symmetry called *R-parity* is conserved [42]. R-parity can be defined as $R = (-1)^F(-1)^{3(B-L)}$ where $F = 1$ for fermions and 0 for bosons, B is baryon number and L is lepton number [36]. Supersymmetric particles have $R = -1$ and Standard Model particles (including all Higgs bosons) have $R = +1$. In this case supersymmetric particles are only produced in pairs, and can therefore only decay into another supersymmetric particle (plus non-supersymmetric particles). Then the lightest supersymmetric particle (LSP) is stable. If the LSP is neutral and not strongly interacting, then it is the perfect candidate for the “dark matter” in the universe. Calculations have shown that there are large regions in the supersymmetric parameter space where the LSP has the right mass and coupling strength to explain the abundance of dark matter [43].

These features, however, have a prize. In the Minimal Supersymmetric extension to the Standard Model (MSSM) [44], which has the smallest possible particle spectrum for a supersymmetric theory, there are still more than 100 new parameters introduced [45], as well as more than a doubling of the number of particles. The number of parameters can be reduced using assumptions concerning the theory at the GUT scale; most frequently used is the constrained MSSM (CMSSM) [46] based on so-called gravity-mediation of the supersymmetry breaking, but there are also other scenarios such as gauge-mediation (see *e.g.* [47]) and anomaly-mediation [48]. However, we don’t know which, if any, of these scenarios is relevant, so in order to exclude the

presence of supersymmetry at colliders the searches must anyway take into account all parameters.

A peculiarity with supersymmetric versions of the Standard Model is that they must have (at least) two Higgs doublets. There are two reasons for this:

1. In a supersymmetric Lagrangian, it is not possible to mix complex conjugates of left-handed chiral superfields, such as the $\tilde{\Phi}$ in eq. (2.29), with non-conjugates (see *e.g.* [36]). This means that in order for the Higgs mechanism to give mass to both down-type fields (charged leptons and down-type quarks) and up-type fields (up-type quarks and possibly neutrinos), we need two Higgs doublets, one with hypercharge $Y = 1$ and one with $Y = -1$.
2. In the Standard Model, the so-called ABJ (Adler-Bell-Jackiw), or triangle, anomaly (see *e.g.* [3]) is exactly cancelled. This happens because the sum of hypercharge of all fermions is zero. If we would have supersymmetry with only one Higgs doublet, an extra fermion (the higgsino) would contribute with hypercharge $Y = 1$. Therefore yet another fermion with hypercharge $Y = -1$ is needed, and is indeed introduced with an extra Higgs doublet superfield.

Therefore there are two Higgs doublets in the MSSM. One of the Higgs doublets, Φ_1 , couples only to up-type singlet fields and has $Y(\Phi_1) = -1$, while the other, Φ_2 , couples only to down-type singlet fields and has $Y(\Phi_2) = 1$. Both the Higgs doublets must get vacuum expectation values in order to give mass to both up- and down-type fields:

$$\langle \Phi_1 \rangle_0 = \begin{pmatrix} v_1 \\ 0 \end{pmatrix}, \quad \langle \Phi_2 \rangle_0 = \begin{pmatrix} 0 \\ v_2 \end{pmatrix} \quad (2.39)$$

The relation between the vacuum expectation values (vev's) v_1 and v_2 and the normal Standard Model vev v is

$$(v_1^2 + v_2^2) = \frac{1}{2}v^2 \quad (2.40)$$

which leaves us with one free parameter to determine the two vev's. This is usually taken to be the ratio of the vev's, parameterized by the angle β :

$$\tan \beta = \frac{v_2}{v_1} \quad (2.41)$$

We can choose v_1 and v_2 positive, and so get $\tan \beta > 0$.

With two Higgs doublets, we have in total eight scalar degrees of freedom. After the electroweak symmetry breaking, three of these are absorbed into the longitudinal components of the three massive vector fields, leaving five

physical Higgs particles. In the absence of CP violation, these are:

$$\begin{aligned}
h, & \quad \text{the lighter neutral } CP\text{-even scalar} \\
H, & \quad \text{the heavier neutral } CP\text{-even scalar} \\
A, & \quad \text{a neutral } CP\text{-odd scalar} \\
H^\pm, & \quad \text{a charged scalar and its antiparticle}
\end{aligned} \tag{2.42}$$

In the MSSM, all properties of these five scalars are given by two parameters at tree-level. These are usually taken to be $\tan\beta$ and the mass of the CP -odd scalar, m_A . The other parameters are then given by

$$m_A^2 = m_{H^+}^2 - m_W^2 \tag{2.43a}$$

$$m_{H,h}^2 = \frac{1}{2} \left[m_A^2 + m_Z^2 \pm \sqrt{(m_A^2 + m_Z^2)^2 - 4m_A^2 m_Z^2 \cos^2 2\beta} \right] \tag{2.43b}$$

$$\cos 2\alpha = -\cos 2\beta \left(\frac{m_A^2 - m_Z^2}{m_H^2 - m_h^2} \right) \tag{2.43c}$$

$$\sin 2\alpha = -\sin 2\beta \left(\frac{m_H^2 + m_h^2}{m_H^2 - m_h^2} \right) \tag{2.43d}$$

where eq. (2.43c)-(2.43d) determines the mixing angle α in the mass matrix of the two neutral CP -even scalars h and H .

Eq. (2.43b) gives an upper bound on the lightest neutral Higgs boson mass $m_h \leq m_Z$ at lowest order. This bound can be relaxed by higher loop corrections to $m_h \lesssim 130$ GeV [49].

At higher orders, the properties of the supersymmetric particles must be taken into account, since they make contributions in loop diagrams. However, there are no more parameters related to the Higgs sector.

2.3.2 General two-Higgs-doublet models²

As discussed above, the introduction of extra Higgs fields can be considered a minimal extension of the Standard Model, and there are a number of possible motivations for doing so (see ref. [1-6] of [51] for examples). It can be shown that as long as the new fields are in the form of doublets and singlets under $SU(2)_L$, the ρ parameter mentioned in sec. 2.1.4 is still $\rho = 1$ at tree-level, which is important because the experimental constraints on this parameter are quite strong. There are also restrictions on the models from the experimental absence of Flavour Changing Neutral Currents (FCNC's), which are absent at tree-level in the minimal Standard Model: A theorem by Glashow and Weinberg [52] states that there will be no FCNC's if all fermions of a given

²For this section I generally refer to [50], chapter 4, for references and further discussion.

electric charge couple to no more than one Higgs doublet. Two examples of two-Higgs-doublet models (2HDM's) with such arrangements are the type II models, where one Higgs doublet (with hypercharge $Y = 1$) couples only to down-type fermions and the other doublet (with $Y = -1$) couples only to up-type fermions, and the type I models, where one of the Higgs doublets couples only to the vector bosons, while the other doublet couples to fermions in the same way as in the minimal Standard Model. As seen above, supersymmetric 2HDM models are of type II.

For a general 2HDM, the Higgs sector will (in the absence of CP violation) still have the Higgs particle spectrum of eq. (2.42), but will have a larger number of parameters. In this case, the Higgs sector has seven free parameters [53]: the four Higgs boson masses, the ratio of vacuum expectation values for the doublets ($\tan \beta$), the mass mixing angle α for the neutral CP -even Higgs bosons and one parameter connected to the three-Higgs boson coupling (see [51] for an exhaustive account of the parameters of general 2HDM's). Before symmetry breaking, the couplings of the Higgs fields to the gauge vector bosons are the same as for the Higgs doublet in the minimal Standard Model, except that in the type II model, one of the Higgs doublet has $Y = -1$. After symmetry breaking, the coupling depends on the vacuum expectation values of the Higgs doublets and on the mixing angle α , such that the couplings of the different physical Higgs particles will be different. The couplings to the fermions are given by the type of 2HDM and the angles α and β . In the case of a type II model we get for the neutral Higgs boson-fermion couplings:

$$\begin{aligned}
H^0 t\bar{t} &: \frac{\sin \alpha}{\sin \beta} & H^0 b\bar{b} &: \frac{\cos \alpha}{\cos \beta} \\
h^0 t\bar{t} &: \frac{\cos \alpha}{\sin \beta} & h^0 b\bar{b} &: \frac{-\sin \alpha}{\cos \beta} \\
A^0 t\bar{t} &: \cot \beta & A^0 b\bar{b} &: \tan \beta
\end{aligned} \tag{2.44}$$

relative to the Standard Model Higgs boson-fermion couplings, while for the charged Higgs boson coupling to t and b we have

$$g_{H^- t\bar{b}} = \frac{g}{2\sqrt{2}m_W} [m_t \cot \beta (1 + \gamma_5) + m_b \tan \beta (1 - \gamma_5)] \tag{2.45}$$

These relations are valid also in the MSSM.

In a general model, the masses of the Higgs particles are independent, in contrast to the supersymmetric model. However, the unitarity bound for vector boson scattering, mentioned in the discussion following eq. (2.37), is still valid, and sets an upper limit on the mass of the lightest neutral Higgs particle, as well as constraints on masses of the other Higgs particles [54]. In the supersymmetric case however, there is a much tighter theoretical upper bound for the lightest neutral Higgs mass, as discussed above.

3. QCD and parton density functions

In the previous chapter, I gave an introduction to the Standard Model of particle physics. However, I focused on the electromagnetic and weak interaction part of the model, and disregarded the strong interaction. The reason for this was that the $SU(3)_c$ group of the strong interaction decouples from the electroweak $SU(2)_L \times U(1)_Y$ group. The strong $SU(3)$ gauge bosons do not couple to the Higgs field, and there is therefore no mixing between the strong bosons and the electroweak bosons. The quarks do couple to the electroweak interaction, but that doesn't affect their behaviour under $SU(3)_c$ interactions.

The theory of the strong interaction is called *quantum chromodynamics* or *QCD*. It has the nice feature that its gauge group, colour $SU(3)$, is not broken. This means that the $SU(3)_c$ symmetry is exactly manifest in nature, just like the electromagnetic $U(1)_Q$ symmetry. However, this doesn't mean that the study of the strong interaction is simpler than the study of the electroweak interaction. In fact, the strong interaction has an enormously rich phenomenology, exhibiting features such as confinement and asymptotic freedom, not to mention the hundreds of hadrons whose properties are not yet fully understood. My research has focused on two special aspects of hadrons, namely *parton density functions*, which is a fascinating area of research because it is on the border between hadronic (non-perturbative) physics and perturbative QCD, and heavy particle production in high-energy hadron collisions, which is closely connected with parton interactions, as will be seen in the following.

In this chapter, after a short introduction to the concepts of perturbative and non-perturbative QCD, I will give an introduction to the parton densities and QCD evolution (the DGLAP equations). I will also discuss some non-perturbative approaches to processes with low momentum transfer, and finally discuss the importance of QCD and parton densities in the search for new physics.

3.1 Perturbative and non-perturbative QCD

According to the systematisation of the hadrons made by Gell-Mann [55] and Zweig [56], baryons, such as the proton and neutron, consist of three quarks, while mesons, *e.g.* the pion, are interpreted as bound states of a quark and an antiquark. To explain this behaviour, the strong force holding the quarks to-

gether in the hadrons should reflect a threefold symmetry. This was done by giving the quarks three different strong charges, *i.e.* sources for the force field of the strong interaction, in contrast to the electromagnetic interaction which has only one charge (and its anticharge). This new quantum number was called *colour*, alluding to the fact that it takes three colours to get a white (colourless) object [57]. The three charges are often called “red, green and blue”. To account for the mesons, each colour charge also has an anticharge (“cyan, magenta and yellow”), such that a colour and its anticolour again makes up an object with no net colour charge. Mathematically, this corresponds to a local gauge symmetry with the non-Abelian gauge group $SU(3)$, which gives the basis for quantum chromodynamics, QCD.

Since QCD is a local gauge theory with a non-Abelian gauge group, it is similar to the $SU(2)_L$ theory of the weak interaction described in chapter 2, sec. 2.1.2. Just as in $SU(2)_L$, the gauge bosons of the $SU(3)_c$ group have self-interactions, although they are massless since the symmetry is not broken. These gauge bosons are called “gluons”, since they “glue” the quarks together into hadrons. One of the most important properties of QCD is *asymptotic freedom*, which was discovered by Gross, Wilzcek and Politzer in 1973 [58]. It means that in the limit of large momentum transfer, the strong interaction coupling tends to zero, so that the quarks seem to be asymptotically free inside the hadrons, as will be discussed in the next section. The fact that the strong coupling α_s becomes small at large momentum transfer allows us to do perturbative expansions in powers of α_s , and in this way calculate scattering processes in QCD.

Processes with small momentum transfer are not as well understood, since there the coupling is too large to allow perturbative calculations. When it comes to such hadronic properties as masses, decays and low-energy interactions, we are in a purely non-perturbative regime, where the large coupling makes a normal perturbative treatment impossible. There, very different methods must be used, such as chiral perturbation theory, where the expansion is made in momenta instead of α_s , see *e.g.* [59], computer simulations using a discretized space-time (lattice QCD; for an introduction see *e.g.* [60]), or models such as those described in sec. 3.3. Lattice simulations are based on the Lagrangian of QCD, and results seem to indicate that QCD is the correct description of the strong interaction also in the non-perturbative regime [61]. In this regime, we encounter completely new phenomena, such as *confinement*, meaning that the colourful quarks are confined in colour-neutral hadrons. The fact that only the colourless hadrons are observed as free particles in nature implies that there must be some mechanism that forbids free colour charges. This mechanism is not yet understood on an analytical level, but lattice simulations have shown that the $SU(3)$ gauge symmetry indeed seems to create confinement [62].

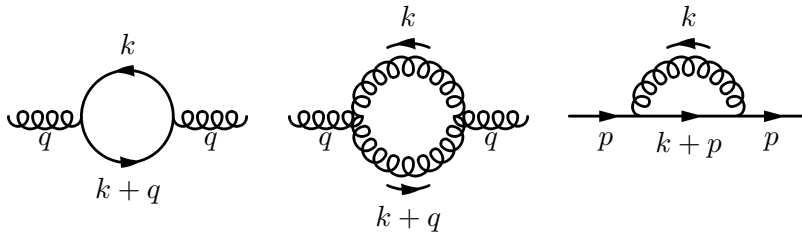


Figure 3.1: Examples of loop diagrams. The plain lines symbolise quarks, while the curly lines correspond to gluons. All letters are four-momenta, going toward the right if not indicated otherwise. In diagrams like these, the momentum k of the particle in the loop isn't restricted by external momenta, leading to infinite integrals which need to be regularised.

3.1.1 Running of couplings and asymptotic freedom¹

When we want to calculate a process at higher orders in perturbation theory, we encounter loops such as those shown in fig. 3.1. In a loop diagram, the momentum of the loop field is not restricted by the external momenta. The reason is that, although there is momentum conservation in every vertex, it enters each vertex twice with opposite signs, giving expressions like $q + k - k = q$. This means that we must integrate over all possible momenta, which often leads to infinite integrals. One way to handle these integrals mathematically is to change the number of space-time dimensions in the calculation, so called *dimensional regularisation* [64]. Going back to the limit of four dimensions, the infinities are isolated in certain terms, which can be absorbed into the couplings and masses of the theory. This means that the “bare” couplings and masses of the Lagrangian (*cf.* eq. (2.3)) are modified by new, infinite contributions. However, only the final, modified parameters are observable in experiments, and so the value of the bare parameters have no physical meaning. A theory is called “renormalisable” if all such infinities can be absorbed into the original parameters of the theory to all orders in perturbation theory. In a non-renormalisable theory, extra parameters must be added for each new calculated order, giving (in principle) infinitely many parameters of the theory. This is the reason why the proof of renormalisability of the Standard Model was such an important achievement (see Chapter 2, sec. 2.1.1).

In the process of renormalisation of the couplings and masses of the theory, a new mass scale must be introduced, called the *renormalisation scale*, μ . In dimensional regularisation, this mass scale is introduced to keep the coupling dimensionless even though the dimension is changed in the integrals. This mass scale is in principle arbitrary, but in a fixed-order calculation there is a residual dependence on the scale chosen, that gets weaker for every new order

¹In this section I refer to [63] for details and references.

in perturbation theory (see sec. 3.4.2 for further discussion of these scales).

However, the couplings and masses of the theory have a real scale dependence, which is not just an artifact. This means that the couplings and masses will have different values depending on the momentum or mass scale of the process we observe. The renormalisation scale μ should then be identified with some scale relevant for the process at hand, usually the momentum transfer or the mass of some heavy particle produced in the process. This dependence is called *running* of masses and couplings. The running of the three couplings of the Standard Model gauge group was shown in fig. 2.4. As is seen in that figure, the manner of the running depends on the particle content of the theory, because with different particle content we get different contributions to the higher-order loop diagrams.

Using the fact that the unrenormalised, “bare” coupling g of the original Lagrangian should not depend on the renormalisation scale, it is possible to derive the scale dependence from the *renormalisation group equations* (see e.g. [3]):

$$\mu \frac{dg_R}{d\mu} = -\frac{\mu}{Z_g} \frac{dZ_g}{d\mu} g_R = \beta(g_R) \quad (3.1)$$

This is the famous beta function. Here g_R is the renormalised coupling and Z_g is the renormalisation factor, which can be calculated from the loop diagrams of the theory. In a given theory we can now (in principle) calculate the beta function to any given order in the coupling.

In QCD, or more generally a gauge theory with gauge group $SU(N)$ (where $N = 2, 3, \dots$), the beta function turns out to be

$$\beta(g) = \beta_0 g^3 + O(g^5) \quad (3.2)$$

with the constant β_0 of the leading (one-loop) term given by

$$\beta_0 = -\frac{1}{(4\pi)^2} \frac{11C_G - 4T_R N_f}{3} = -\frac{1}{(4\pi)^2} \frac{33 - 2N_f}{3} \text{ for QCD } (N=3) \quad (3.3)$$

where N_f is the number of quark flavours. Using the standard method of separation of variables we can easily solve the differential equation (3.1) for g_R (for simplicity we drop the subscript R on g):

$$\frac{d\mu}{\mu} = \frac{dg}{\beta(g)} \implies \ln\left(\frac{\mu}{\mu_0}\right) = \int_{g(\mu_0)}^{g(\mu)} \frac{dg'}{\beta(g')} \approx \frac{1}{2\beta_0} \left(\frac{1}{g_0^2} - \frac{1}{g(\mu)^2} \right) \quad (3.4)$$

where in the last step the one-loop result was inserted. μ_0 is the starting scale

of the evolution.

Now, the behaviour of the coupling depends on the behaviour of the β function. If $\beta > 0$ for all g , then the coupling will grow indefinitely with growing momentum scale t , until perturbation theory is no longer valid. This happens in QED, and the limit where the coupling diverges is called the Landau pole [65]. If, however, $\beta < 0$ at least for small g , the coupling will instead get smaller when the momentum scale grows, finally approaching zero. This behaviour is called *asymptotic freedom*. The discovery of asymptotic freedom in QCD in 1973 [58] was fundamental to the understanding of the strong force.

For small g , $\beta < 0$ if $\beta_0 < 0$. In QCD, this is true for $N_f < 33/2$, which is well satisfied in the Standard model where there are six quark flavours, u , d , s , c , b and t . The two terms in eq. (3.3) correspond to the contribution to the β function from the gluon self-couplings and the quark-gluon couplings, respectively. We see that it is the gluon self-interactions, *i.e.* the non-Abelian property of the interaction, that gives rise to asymptotic freedom.

For the strong coupling $\alpha_s = g^2/4\pi$ we get

$$\alpha_s(\mu^2) = \frac{4\pi}{(11 - 2N_f/3) \ln(\mu^2/\Lambda^2)} \quad (3.5)$$

The new scale $\Lambda = \mu_0 e^{1/(2\beta_0 g^2)}$ is a characteristic scale of the strong interaction, and is the only adjustable parameter in QCD except for the quark masses. It is the QCD equivalent of the Landau pole of QED. However, in QED, the Landau pole is in the ultraviolet (high-momentum) region, while in QCD the pole is in the infrared (low-momentum) region. In order to be able to use perturbation theory, we need to make sure that our calculations are done in a momentum region where $\mu^2 \gg \Lambda^2$. The value of Λ_{QCD} is of the order [66]

$$\Lambda_{\text{QCD}} \sim 100 - 400 \text{ MeV} \quad (3.6)$$

depending on the number of effective quark flavours. In practise, perturbative calculations seem to be valid down to $\mu^2 \sim 1 \text{ GeV}^2$ [67].

In this section we have made the calculation of the running of α_s to one-loop order, but eq. (3.1) can be solved (in principle) to any order. For QCD, the beta function has so far been calculated to four-loop order [69]. At the Z mass scale, the world average experimental value for α_s is [68]:

$$\alpha_s(M_Z^2) = 0.1182 \pm 0.0027 \quad (3.7)$$

A recent plot showing the running of the strong coupling $\alpha_s = g_s^2/4\pi$ is given in fig. 3.2.

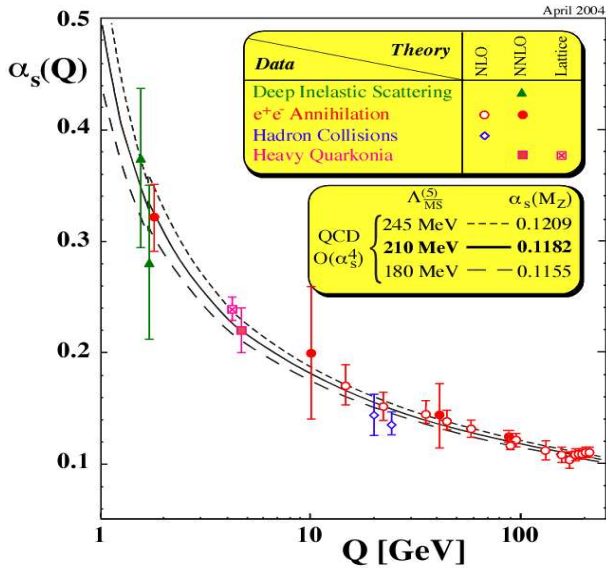


Figure 3.2: Summary of measurements of the strong coupling parameter $\alpha_s(Q^2)$ as of 2004, from [68]. The decrease of α_s with increasing scale is very well described by QCD with basically only one parameter, Λ_{QCD} . We also see from the figure that soon below 1 GeV the coupling becomes unity, effectively making perturbation theory impossible.

3.2 Parton density functions

The word “parton” was first used by Feynman for the point-like constituents (parts) of the proton. This means that the word is used collectively for the quarks, antiquarks and gluons in a hadron. Although the quantum numbers of a baryon can be described using only three valence quarks, these are only one component of the hadron. A large part of the hadron momentum is taken by gluons, and there is also a “sea” of quarks and antiquarks, which don’t contribute to the charge or isospin quantum numbers of the hadron. The probability to find a parton in a hadron can be parameterised by *parton density functions* (also called *parton distribution functions*). Parton densities have a special status in that they are at the border between the perturbative and non-perturbative regions; some aspects of the parton densities (the Q^2 -evolution in particular) can be perturbatively calculated to high precision, while others (e.g. the full x -dependence) is non-perturbative and cannot be calculated from first principles (*i.e.* from the QCD Lagrangian).

Deep inelastic scattering (DIS), *i.e.* lepton-nucleon collisions with large momentum transfer between the lepton and the nucleon, is the main tool to get information on parton density functions, and I will therefore start by dis-

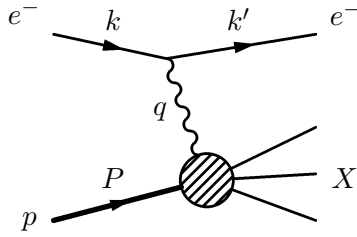


Figure 3.3: Deep inelastic electron-nucleon scattering. k , k' , q and P are four-momenta.

cussing these in some detail.

3.2.1 Deep inelastic scattering²

A deep inelastic scattering experiment consists in using a high-energy lepton to probe the structure of a nucleon (or nuclear) target, as depicted in fig. 3.3. In so-called *inclusive* experiments, only the scattered lepton is observed. Therefore the formalism for inclusive DIS doesn't depend on the details of the hadronic final state, denoted by X in fig. 3.3. To be specific, I will in the following focus on electron-proton scattering, although all results remain identical for scattering with any charged lepton. In neutrino-nucleon scattering however, some new features appear, see e.g. [70].

With the four-momenta given in fig. 3.3 (k for the incoming electron, k' for the scattered electron, $q = k - k'$ for the virtual photon and P for the proton with mass M), we have the following standard kinematical variables in DIS:

$$Q^2 = -q^2 \quad (3.8a)$$

$$\nu = \frac{P \cdot q}{M} = E - E' \quad (3.8b)$$

$$x = \frac{Q^2}{2M\nu} = \frac{Q^2}{2M(E - E')} \quad (3.8c)$$

$$y = \frac{q \cdot P}{k \cdot P} = 1 - E'/E \quad (3.8d)$$

Here, the second equalities refer to the frame where the proton is at rest, with $E = k^0$ and $E' = k'^0$. The variable x is called Bjorken- x . x and y are kinematically constrained to be between 0 and 1. Note that there are different conventions for the definition of ν , sometimes $\nu = P \cdot q$ is used (with $x = Q^2/2\nu$ still dimensionless).

The cross-section for charged lepton-proton scattering $l^\pm p \rightarrow l^\pm X$ can be

²In these sections I follow to a large extent [70].

written as

$$\frac{d^2\sigma^{em}}{dx dQ^2} = \frac{4\pi\alpha^2}{Q^4} \left[y^2 F_1(x, Q^2) + \frac{1}{x} \left(1 - y - \frac{M}{2E} xy \right) F_2(x, Q^2) \right] \quad (3.9)$$

F_1 and F_2 are called the proton *structure functions*, and are associated with the electromagnetic form factors, defined by conservation of the electromagnetic current. I have omitted a third structure function, F_3 , which is associated with the parity-breaking weak interaction, and can be neglected for charged lepton scattering at momentum transfers Q^2 clearly below $M_Z^2 \sim 8000 \text{ GeV}^2$. For neutrino scattering, the corresponding term F_3^ν is important at all scales.

Since we are interested in scattering with high-energy electrons, where $E \gg M$, we can neglect the last term in eq. (3.9). We can also define the *longitudinal structure function* F_L as

$$F_L(x, Q^2) = \left(1 + \frac{4M^2 x^2}{Q^2} \right) F_2(x, Q^2) - 2x F_1(x, Q^2) \quad (3.10)$$

F_L corresponds to the absorption of longitudinally polarised (virtual) photons, while F_1 corresponds to absorption of transversely polarised photons. Obviously, $F_L \rightarrow F_2 - 2x F_1$ when $Q^2/x^2 \gg M^2$. We can then write eq. (3.9) as

$$\frac{d^2\sigma^{em}}{dx dQ^2} = \frac{4\pi\alpha^2}{Q^4} \left[[1 + (1 - y)^2] F_1 + \frac{1 - y}{x} F_L \right] \quad (3.11)$$

In the naive parton model, the proton is composed of point-like, massless, non-interacting partons with spin $\frac{1}{2}$. The differential cross-section for scattering of a charged lepton off such a parton is given by

$$\frac{d\hat{\sigma}}{dQ^2} = \frac{2\pi\alpha^2 e_q^2}{Q^4} [1 + (1 - y)^2] \quad (3.12)$$

where the ‘‘hat’’ ($\hat{\cdot}$) on σ is to indicate lepton-parton scattering and e_q is the fractional charge of the parton. Note that for such spin- $\frac{1}{2}$ partons, $F_L = 0$. This is called the *Callan-Gross relation* [71].

In eq. (3.12), there is no dependence on x . In order to find the x -dependence, and at the same time get an interpretation for this variable, we go to the *infinite momentum frame*, in which the proton is moving with a very large momentum $P^\mu = (P, 0, 0, P)$ ($P \gg M$, so that the proton can be considered to be massless). In this frame, the transverse momenta of the partons are small relative to their momenta in the direction of the proton momentum, since all partons are moving together with the proton. This means that the momentum of a parton

can be written as

$$p^\mu = \xi P^\mu = (\xi P, 0, 0, \xi P) \quad (3.13)$$

where $0 < \xi < 1$. If we now let this parton be struck by the virtual photon (see fig. 3.4a) and constrain the incoming and outgoing momenta to be on the mass shell $p^2 = p'^2 = 0$,

$$0 = p'^2 = (p + q)^2 = p^2 + 2p \cdot q + q^2 = 2\xi P \cdot q - Q^2 = 2M\nu(\xi - x) \quad (3.14)$$

we get $\xi = x$, so that x can be identified with the momentum fraction carried by the struck parton. Note that the so-called *light-cone* x , $x_{\text{LC}} = p_+/P_+ = (E + p_z)/(E_P + P_Z)$ where E_P is the energy of the proton, is also equivalent to Bjorken- x in the infinite-momentum frame.

From these considerations, we get for charged lepton scattering on a point-like spin- $\frac{1}{2}$ parton in the infinite-momentum frame

$$\frac{d\hat{\sigma}}{dx dQ^2} = \frac{4\pi\alpha^2}{Q^4} [1 + (1 - y)^2] \frac{1}{2} e_q^2 \delta(x - \xi) \quad (3.15)$$

Comparing this with eq. (3.11), we see that for a point-like parton,

$$\hat{F}_L = \hat{F}_2 - 2x\hat{F}_1 = 0 \quad (3.16)$$

$$\hat{F}_2(x, Q^2) = 2x\hat{F}_1(x, Q^2) = xe_q^2 \delta(x - \xi) \quad (3.17)$$

Let us now assume that the photon scatters incoherently off the partons in the proton, and that we have the probability distribution $q(\xi)$ to find the quark q at momentum fraction ξ in the proton. We then get (in the naive parton model)

$$F_2(x, Q^2) = 2xF_1 = \sum_{q, \bar{q}} \int_0^1 d\xi q(\xi) xe_q^2 \delta(x - \xi) = \sum_{q, \bar{q}} xe_q^2 q(x) \quad (3.18)$$

and we see that the structure functions *scale*, *i.e.* do not depend on Q^2 , if we change ν and Q^2 in such a way as to keep x fixed. This is called Bjorken scaling [72]. Experimentally, Bjorken scaling was discovered at the Stanford Linear Accelerator Center in California [73], proving that the proton indeed was made of point-like constituents. The property $F_2 \simeq 2xF_1$ (the Callan-Gross relation) was a strong test of the spin- $\frac{1}{2}$ nature of the quarks.

By comparing different scattering experiments, such as electron-proton, electron-deuteron (assuming isospin symmetry between the proton and neu-

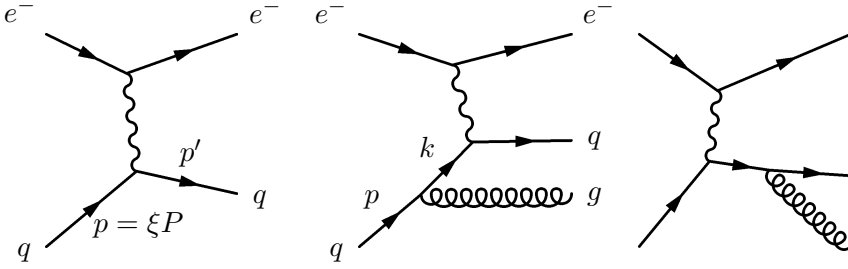


Figure 3.4: Scattering of an electron on a parton in the proton (a) to leading order; (b) and (c) taking into account the radiation of a gluon from the struck quark. In (b), the momenta are related by $k = zp = xP$ and $p = \frac{x}{z}P$.

tron such that $u^p(x) = d^n(x)$ and $d^p(x) = u^n(x)$) and neutrino-nucleon scattering, it is possible to get sum rules for the different quark and antiquark species in the proton, enabling the extraction of the individual quark density functions from experiments.

If we go beyond the naive parton model, and take the interactions between quarks and gluons predicted by QCD into account, then Bjorken scaling is no longer exact but is broken by logarithms of Q^2 . This will be discussed in the next section.

3.2.2 QCD corrections to parton densities

One of the first and most powerful tests of QCD is the logarithmic scaling violations observed in deep inelastic scattering. We will now see how these scaling violations arise. In QCD, there is a possibility for the quark to radiate a gluon in connection to being struck by the virtual photon. These processes are shown in fig. 3.4.

The leading order process (fig. 3.4a) was calculated in the previous section (for simplicity of notation, we put $\xi = 1$ in the following):

$$\hat{F}_2(x) = xe_q^2 \delta(1-x) \quad (3.19)$$

If we calculate the contribution from the gluon radiation processes shown in fig. 3.4b and c and integrate over all allowed values of the gluon momentum $(p - k)$, we find that this integral has a component

$$\hat{F}_2(x) \Big|_{\text{div}} = e_q^2 \frac{\alpha_s}{2\pi} xP(x) \int_0^{2M\nu} \frac{d|k^2|}{|k^2|} \quad (3.20)$$

This integral is logarithmically divergent in the infrared (as the quark vir-

tuality $k^2 \rightarrow 0$). We must therefore cut it off at some low virtuality $k^2 = \kappa^2$, and obtain for the structure function

$$\hat{F}_2(x, Q^2) = e_q^2 x \left[\delta(1-x) + \frac{\alpha_s}{2\pi} \left(P(x) \ln \frac{Q^2}{\kappa^2} + C(x) \right) \right] \quad (3.21)$$

The functions $P(x)$ and $C(x)$ can be calculated from the squared sum of the diagrams 3.4b and c. However, we are mostly interested in $P(x)$ since that is the term which gives rise to the scaling violations:

$$P(x) = \frac{4}{3} \frac{1+x^2}{1-x} \quad (3.22)$$

for $x < 1$ (at $x = 1$, $P(x)$ is regularised in such a way that $\int_0^1 P(x) dx = 0$ in order to conserve the quark number in the proton).

For the proton structure function we now get

$$F_2(x, Q^2) = \sum_{q, \bar{q}} x e_q^2 \left[q_0(x) + \frac{\alpha_s}{2\pi} \int_x^1 \frac{dz}{z} q_0\left(\frac{x}{z}\right) \left\{ P(z) \ln \frac{Q^2}{\kappa^2} + C(z) \right\} \right] \quad (3.23)$$

where $q_0(x)$ is the bare quark density and $z = k/p$ is the fraction of the original longitudinal momentum of the quark transferred to the quark after the emission of the gluon in fig. 3.4b.

Here we seem to have a problem: it appears that the physics should be very sensitive to the infrared cutoff κ^2 . Fortunately, this is not the case. The solution is that the bare quark density $q_0(x)$ in eq. (3.23) is not a physical observable. This means that we can absorb the divergence into a renormalised quark density q :

$$q(x, \mu^2) = q_0(x) + \frac{\alpha_s}{2\pi} \int_x^1 \frac{dz}{z} q_0\left(\frac{x}{z}\right) P(z) \ln \frac{\mu^2}{\kappa^2} \quad (3.24)$$

The scale μ^2 is called the *factorisation scale*. It is the scale at which the quark density is evaluated. The resulting expression for F_2 becomes

$$F_2(x, Q^2) = \sum_{q, \bar{q}} x e_q^2 \left[q(x, \mu^2) + \frac{\alpha_s}{2\pi} \int_x^1 \frac{dz}{z} q\left(\frac{x}{z}, \mu^2\right) \times \right. \\ \left. \times \left\{ P(z) \ln \frac{Q^2}{\mu^2} + C(z) + \dots \right\} \right] \quad (3.25)$$

where “+ ...” signifies higher-order terms (in α_s). Depending on which finite

terms we absorb into the quark density and which terms we leave in F_2 we get different *factorisation schemes*, because it corresponds to different ways to factorise the parton description from the hard scattering (the scattering with the largest momentum transfer). As long as we are consistent in our treatment, the choice of factorisation scheme doesn't affect the physical results. The most common factorisation scheme is called $\overline{\text{MS}}$ (modified minimal subtraction scheme or "MS-bar") [74]. See *e.g.* [2, 63, 75] for details.

Note that if we set $\mu^2 = Q^2$ in eq. (3.25), the logarithm $\ln(Q^2/\mu^2) = 0$ so that all Q^2 -dependence resides in the quark densities $q(x, Q^2)$. This is the standard choice for the factorisation scale in DIS. With more complicated final states, the precise choice of factorisation scale is no longer as obvious. This will be discussed in sec. 3.4.2.

3.2.3 The DGLAP equations

Eq. (3.24) shows the dependence of the quark density on the factorisation scale to leading order in α_s . However, this order is not enough. The reason is that although α_s is small, the logarithm $\ln(\mu^2/\kappa^2)$ can be large. Therefore the combination $\frac{\alpha_s}{2\pi} \ln(\mu^2/\kappa^2)$ need not be small, especially since the inversely logarithmic scale dependence of α_s (see sec. 3.1.1) is compensated by the logarithm. To account for this, we would like to make a *resummation* of all terms which are proportional to $\frac{\alpha_s}{2\pi} \ln(\mu^2/\kappa^2)$ to some power n . Such a resummation is said to be to *leading logarithmic order*.

Let us now see how the multiple logarithms arise in the case of the quark density (3.24). As a preparatory step, we rewrite eq. (3.24) as an integral over the virtuality $t' = k^2$ from $t_0 = \kappa^2$ to $t = \mu^2$:

$$q(x, t) = q_0(x) + \int_{t_0=\kappa^2}^{t=\mu^2} \frac{dt'}{t'} \frac{\alpha_s}{2\pi} \int_x^1 \frac{dz}{z} P(z) q_0\left(\frac{x}{z}\right) \quad (3.26)$$

This is the expression for the quark density resulting from the emission of one gluon at virtuality $t' < t$. Now, we can imagine that the quark has previously radiated another gluon at a scale t'' , $t_0 < t'' < t'$. Retracing our

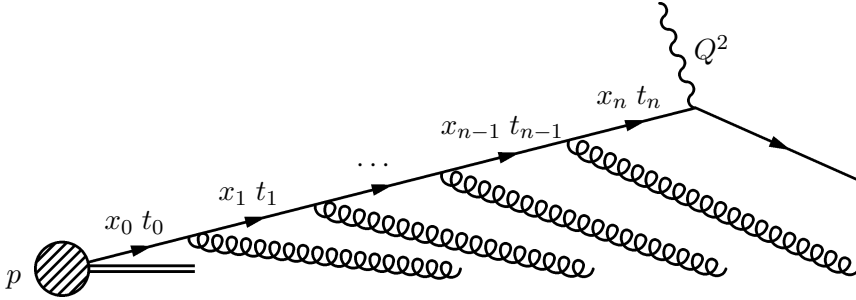


Figure 3.5: The struck quark radiating several gluons at successive t and x , such that $t_0 \ll t_1 \ll \dots \ll t_{n-1} \ll t_n \ll t = Q^2$ and $x_0 > x_1 > \dots > x_{n-1} > x_n = x$.

steps, we see that such a radiation would result in

$$\begin{aligned}
 q(x, t) &= q_0(x) + \int_{t_0}^t \frac{dt'}{t'} \frac{\alpha_s}{2\pi} \int_x^1 \frac{dz}{z} P(z) \left\{ q_0\left(\frac{x}{z}\right) + \right. \\
 &\quad \left. + \int_{t_0}^{t'} \frac{dt''}{t''} \frac{\alpha_s}{2\pi} \int_{x/z}^1 \frac{dz'}{z'} P(z') q_0\left(\frac{x}{zz'}\right) \right\} = \\
 &= q_0(x) + \frac{\alpha_s}{2\pi} \ln\left(\frac{t}{t_0}\right) \int_x^1 \frac{dz}{z} P(z) q_0\left(\frac{x}{z}\right) + \\
 &\quad + \frac{1}{2!} \left[\frac{\alpha_s}{2\pi} \ln\left(\frac{t}{t_0}\right) \right]^2 \int_x^1 \frac{dz}{z} P(z) \int_{x/z}^1 \frac{dz'}{z'} P(z') q_0\left(\frac{x}{zz'}\right) \approx \\
 &\approx q_0(x) + \int_{t_0}^t \frac{dt'}{t'} \frac{\alpha_s(t')}{2\pi} \int_x^1 \frac{dz}{z} P(z) q\left(\frac{x}{z}, t'\right)
 \end{aligned} \tag{3.27}$$

where the last step follows from the first, and the middle equality is only inserted to show the appearance of the $\left[\frac{\alpha_s}{2\pi} \ln\left(\frac{t}{t_0}\right)\right]^2$ -term.

Note that, in the last step, we evaluate the running coupling $\alpha_s(t)$ (see sec. 3.1.1) at the same scale as the quark distribution function. If we look at more successive gluon radiations at ever decreasing t (see fig. 3.5), we include higher powers of $\left[\frac{\alpha_s}{2\pi} \ln\left(\frac{t}{t_0}\right)\right]$, and the last step in eq. (3.27) turns into an identity. Differentiating with respect to t , we get the famous DGLAP (Dokshitzer-Gribov-Lipatov-Altarelli-Parisi) equation [76] (which is often just called the Altarelli-Parisi equation):

$$\frac{\partial q(x, t)}{\partial \ln t} = \frac{\alpha_s(t)}{2\pi} \int_x^1 \frac{dz}{z} P(z) q\left(\frac{x}{z}, t\right) \tag{3.28}$$

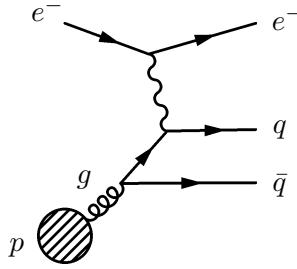


Figure 3.6: Splitting of a gluon from the proton into a quark-antiquark pair, where the quark subsequently interacts with the electron.

This equation determines the QCD evolution of the quark density as the momentum transfer scale changes. It can be solved numerically with standard methods. However, there are a couple of points I would like to stress:

- The DGLAP equation (3.28) is a differential equation in t . This means that we must introduce an initial condition at some scale t_0 , *i.e.* a starting distribution. The x -shape of these starting quark and gluon distributions (*cf.* $q_0(x)$ in eq. (3.27)) cannot be derived from perturbative QCD, although there are some arguments for their general shape (see *e.g.* [77]). Usually they are taken as more or less arbitrary functions with parameters that are then fitted to experiment. In our papers II-IV, we have tried a different approach and used a physically motivated model giving the shape of the starting distributions, see sec. 3.2.5 below.
- The parton density functions derived here in the context of electron-proton scattering are *universal*. This means that whenever we have a proton in a hard process (*i.e.* a process with large momentum transfer), the probability to “find” a given parton in the proton at a given x and μ^2 is the same, independent of the nature of the interaction. Note that it is important that all calculations are done in the same factorisation scheme, to ensure that all finite terms are taken into account once and only once.
- In the derivation of the DGLAP equation, we only used the logarithmically divergent part of the gluon radiation expression. This corresponds to *soft* and *collinear emissions*, where the relative transverse momentum of the gluon and the quark vanishes. Furthermore, we have only considered successive emissions which are strongly ordered in the virtuality ($t_0 \ll t_1 \ll \dots$), and ordered in x ($x_0 > x_1 > \dots$). These are the leading terms in most of the DIS phase space, and this approximation therefore works exceedingly well to describe data. However, at very small x , new terms including factors of $\ln(1/x)$ should become important. Resummation of such terms results in the BFKL equation [78].

So far our treatment has been a bit simplified, in that we have neglected

the contribution to the quark density function from gluon splitting into quark-antiquark pairs which then interact with the electron (see fig. 3.6). The treatment of the gluon splitting is quite similar to the case described above where a quark radiated a gluon. Corresponding to eq. (3.21) above, we get

$$\hat{F}_2^g(x, Q^2) = x \sum_{q, \bar{q}} e_q^2 \frac{\alpha_s}{2\pi} \left(P_{qg}(x) \ln \frac{Q^2}{\kappa^2} + C_g(x) \right) \quad (3.29)$$

Note that the first term here is already at order α_s , since the gluon doesn't interact directly with the photon. $P_{qg}(x)$ should be read as ‘‘the probability to find a quark with a longitudinal momentum fraction x in a gluon’’. It has the form

$$P_{qg}(x) = \frac{1}{2} [x^2 + (1-x)^2] \quad (3.30)$$

This means that the full expression for the quark density to order α_s (cf. eq. (3.24)) is

$$\begin{aligned} q(x, \mu^2) = & q_0(x) + \frac{\alpha_s}{2\pi} \int_x^1 \frac{dz}{z} q_0\left(\frac{x}{z}\right) P_{qq}(z) \ln \frac{\mu^2}{\kappa^2} \\ & + \frac{\alpha_s}{2\pi} \int_x^1 \frac{dz}{z} g_0\left(\frac{x}{z}\right) P_{qg}(z) \ln \frac{\mu^2}{\kappa^2} \end{aligned} \quad (3.31)$$

where I have denoted $P(z)$ in eq. (3.21) by $P_{qq}(z)$ since it corresponds to the probability to find a quark with longitudinal momentum fraction z in a quark.

Now F_2 is given by

$$\begin{aligned} F_2(x, Q^2) = & \sum_{q, \bar{q}} x e_q^2 \left[q(x, Q^2) + \frac{\alpha_s}{2\pi} \int_x^1 \frac{dz}{z} q\left(\frac{x}{z}, Q^2\right) C_q(z) + \dots \right] + \\ & + \sum_{q, \bar{q}} x e_q^2 \left[\frac{\alpha_s}{2\pi} \int_x^1 \frac{dz}{z} g\left(\frac{x}{z}, Q^2\right) C_g(z) + \dots \right] \end{aligned} \quad (3.32)$$

where we have put $\mu^2 = Q^2$ and the exact form of the finite functions $C_q(x)$ and $C_g(x)$ depends on what factorisation scheme we choose. The ‘‘+...’’ signifies higher-order terms in α_s .

For the DGLAP equation (3.28), if we take into account processes such as that in fig. 3.6, we get a linear system of equations connecting the $2N_f$ quark

and antiquark distributions with the gluon distribution:

$$\begin{aligned}
\frac{\partial q_i(x, t)}{\partial \ln t} &= \frac{\alpha_s(t)}{2\pi} \sum_j \int_x^1 \frac{dz}{z} P_{q_i q_j}(z, \alpha_s(t)) q_j(x, t) + P_{q_i g}(z, \alpha_s(t)) g(x, t) \\
\frac{\partial g(x, t)}{\partial \ln t} &= \frac{\alpha_s(t)}{2\pi} \sum_j \int_x^1 \frac{dz}{z} P_{g q_j}(z, \alpha_s(t)) q_j(x, t) + P_{g g}(z, \alpha_s(t)) g(x, t)
\end{aligned}
\tag{3.33}$$

where $i, j = 1, \dots, 2N_f$. Here we have included the possibility for higher order splitting functions dependent on α_s , corresponding to resummations of higher-order logarithms $\left[\left(\frac{\alpha_s}{2\pi} \right)^{n+k} \ln^n \left(\frac{t}{t_0} \right) \right]$. The splitting functions have recently been calculated to 3-loop (next-to-next-to-leading logarithmic) order [79].

3.2.4 Parton showers

In a Monte Carlo event generator, the parton radiation described by the DGLAP equation can be implemented as a means to describe the production of extra QCD jets in a process. This is called *initial state radiation* and *final state radiation*, depending on whether the partons are radiated “before or after” the interaction with the electron, or collectively *parton showers* (see e.g. [80]). The distribution of transverse momenta p_\perp for initial state parton showers is given by eq. (3.33) and the relation $p_\perp^2 = (1 - z)t$ for massless splittings. For final-state parton showers, the dominating contributions are, just as in the case of initial-state radiation, the logarithmically enhanced soft and collinear emissions. Therefore this process is also described by the DGLAP evolution equations, but with the starting quark and gluon distributions of the interacting hadron replaced by the outgoing quark or gluon.

In both initial and final state radiation, the maximum transverse momentum of a radiated parton is then given by the factorisation scale $\mu^2 = Q^2$ (although the probability for an emission to actually have this maximum virtuality is vanishingly small). In practise, a larger maximum scale is often used to effectively include also non-collinear emissions and improve fits to experimental data. From eq. (3.27) we see that the emissions will have strongly ordered, successively smaller transverse momenta as we go backward (in the case of initial state radiation) or forward (for final state radiation) in the emission chain from the hard scattering, as indicated in fig. 3.5. We continue until some lower cut-off is reached, e.g. 1 GeV² [80]. In practical implementations in Monte Carlo showering programs, the probability for a parton emission at a certain scale is given by so-called *Sudakov form factors* (to be precise, the

Sudakov form factor $\Delta(t_1, t_2)$ is the probability for a parton *not* to radiate between the scales t_1 and t_2). For a pedagogical description of how this is done in practise, I refer to [70].

To get a more precise description of jet emission with large transverse momentum, the exact matrix element for the process including this emission must be used, calculated from the Feynman diagrams. However, the naive combination of the exact description with the parton shower description will result in double-counting in the small-transverse momentum region (see sec. 3.4.2). In our papers VI-VII, we developed an algorithm to correct for such double-counting in the case of production of charged Higgs bosons in association with top and bottom quarks in hadron colliders, and implemented the algorithm as a Monte Carlo event generator.

3.2.5 The starting distributions

As mentioned above, the DGLAP equation gives the dependence of the parton densities on the momentum transfer scale of the hard scattering. However, perturbative QCD cannot be used to calculate the *starting distributions*, *i.e.* the parton densities at the scale $Q_0^2 = t_0$ where the DGLAP evolution is started. Instead, they are usually taken as parameterisations of some more or less arbitrary functions, where the parameters are extracted from global fits to experimental data. These functions have become successively more complicated in order to account for new features found in data, such as the excess of large-transverse-energy jets seen in the CDF experiment at the Tevatron in 1995 [81]. This excess turned out to be explainable by a surprisingly large gluon density at large x [82].

One parameterisation, used by the CTEQ collaboration, is [83]

$$xf(x, Q_0) = A_0 x^{A_1} (1-x)^{A_2} e^{A_3 x} (1 + e^{A_4 x})^{A_5} \quad (3.34)$$

with independent parameters for the different distributions ($u_v = u - \bar{u}$, $d_v = d - \bar{d}$, g etc.), in such a way that there are in this case 20 independent shape parameters ($A_1 - A_5$ in eq. (3.34)) in the parameterisation.

Some of the normalisation parameters (A_0 in eq. (3.34)) are fixed by sum rules. These are the quark number sum rule

$$\int_0^1 (q(x) - \bar{q}(x)) dx = N_q \quad (3.35)$$

and the total momentum sum rule

$$\sum_{i=q, \bar{q}, g} \int_0^1 x f_i(x) dx = 1 \quad (3.36)$$

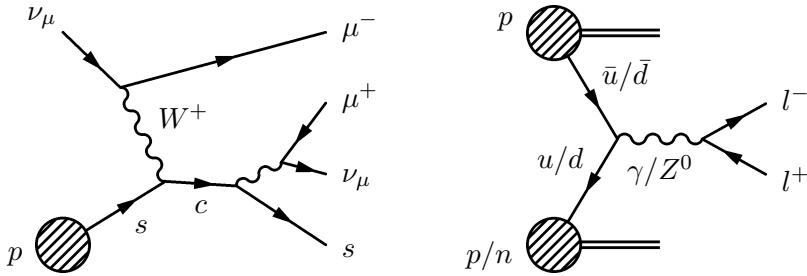


Figure 3.7: (a) Di-muon production in a neutrino experiment. The neutrino interacts with a strange quark in the proton to produce a muon and a c quark, which subsequently decays to a muon of the opposite sign. This process can be used to probe the strange sea in the proton. Note that this process (with a neutrino) is only possible for an s quark, while the corresponding process with an antineutrino is only possible with an \bar{s} quark, due to charge conservation. (b) The Drell-Yan process: production of charged lepton pairs in pp or pn interactions. A u (d) quark from one of the hadrons annihilate with a \bar{u} (\bar{d}) quark from the other to produce a charged lepton pair via a neutral electroweak vector boson. The cross-section is dominated by the u and \bar{u} distributions due to the larger electric charge of the u quark. Comparing production from a pure proton target and a nuclear target containing neutrons, it is possible to extract the \bar{u} distributions of the proton and neutron separately.

These sum rules have very natural interpretations: The integrated net quark density corresponds to the number N_q of q -quarks in the hadron (for the proton, $N_u = 2$ and $N_d = 1$ while $N_s = N_c = N_b = 0$), while the sum of integrated x -weighted parton densities corresponds to the sum of momentum fractions taken by the partons in the hadron. This means that there are independent normalisations only for the light sea quarks (\bar{u} and \bar{d}) and the strange sea ($s + \bar{s}$). The DGLAP equation conserves these sum rules, which can be seen in the case of gluon splitting from eq. (3.33) and (3.30); since P_{qg} is symmetric between the quark and the antiquark, the gluon splitting into $q\bar{q}$ doesn't affect the net quark number, and because the quark and antiquark shares the gluon momentum, the total momentum is not affected. Similar analyses can be done for the process of a quark radiating a gluon, and a gluon splitting into two gluons. The x -distributions of the partons are however changed by the DGLAP evolution, as well as the fractions of the momenta taken by different partons.

Some earlier parameterisations [84] assumed that, at some low scale, the proton consisted only of valence quarks and gluons, and that the sea quarks were generated purely by gluon splitting as described by the DGLAP evolution. If this were the case, the sea should be flavour symmetric, *i.e.* $\bar{u} = \bar{d} = s = \bar{s}$. However, it was found from di-muon production in neutrino experi-

ments [85] (see fig. 3.7a) that

$$\frac{s + \bar{s}}{2} \approx 0.5 \frac{\bar{u} + \bar{d}}{2} \quad (3.37)$$

showing that the sea was not $SU(3)$ symmetric. Furthermore, in Drell-Yan dilepton production it was shown that the \bar{u} and \bar{d} distributions of the proton also differed [86]. This could be seen by comparing the di-lepton production cross-section in proton-proton and proton-nucleus interactions (see fig. 3.7b), and assuming that $\bar{d}^p = \bar{u}^n$. These data showed that $\bar{d}(x) > \bar{u}(x)$ in the proton, indicating a non-perturbative origin of the light sea different from the flavour symmetric gluons splitting. This was anticipated by Field and Feynman [87], who argued that there should be a Pauli suppression in the production of $u\bar{u}$ pairs compared to $d\bar{d}$ pairs due to the larger number of u quarks than d quarks in the proton. There are also other models which predict an asymmetry of this kind, most notably the meson cloud models (see [88] for a review of sea quark asymmetries).

In papers II-IV we present developments of a physically motivated model [89] for both the valence distributions and the sea distributions of the proton, where asymmetries between sea quark distributions are explained by quantum fluctuations of the proton into baryon-meson pairs. This model needs few parameters, and reproduces data both from deep inelastic scattering experiments and from quark asymmetry measurements. In this model we find the expected excess of \bar{u} over \bar{d} . We also find an asymmetry in the strange sea, $\int_0^1 (xs(x) - x\bar{s}(x))dx > 0$, which is of relevance for the so called NuTeV anomaly, discussed in sec. 3.4.1 below. Furthermore, the model suggests the presence of charm quarks in the starting distributions, as discussed in paper IV.

In the region where the perturbative description in terms of uncorrelated scattering of the photon off single partons in the proton does not apply, other methods must be used to describe the scattering. In our paper I, we investigate an alternative description of electron-proton scattering at low Q^2 , namely the VDM formalism, which draws on Regge theory and the hadronic properties of the photon, to be discussed in the next section.

3.3 Non-perturbative processes

Due to asymptotic freedom, it is possible to make quite precise theoretical calculations using perturbative QCD, as long as we are in the regime of high momentum-transfer. However, this is true almost exclusively in high-energy collision events (and to some extent in the decay of heavy hadrons), and even there, there are non-perturbative aspects that need to be taken into account.

These have to do with the properties of hadrons, such as the parton distributions discussed above, the formation of hadrons from the outgoing quarks and gluons, and the calculation of total cross-sections, which are dominated by “soft” processes with low momentum transfer. We then have to resort to either model-building (such as the hadronisation models or the VDM models for photon-hadron interactions), or methods which do not rely on perturbation theory (such as Regge theory).

3.3.1 Hadronisation

After a hard scattering, the quarks and gluons going out from the hard scattering emit partons through final state radiation, as described in sec. 3.2.4 above. This process is continued down to a lower cut-off scale. At this scale, where perturbation theory is no longer applicable, the outgoing partons go over into the colour-neutral hadrons which can be observed in detectors. This process is called *hadronisation*. The precise mechanism of hadronisation is not yet fully understood, and should be intimately connected to the problem of confinement (discussed in sec. 3.1). However, there are models for hadronisation which give a good description of final-state data at colliders, such as the Lund string model [90] and the cluster fragmentation model [91]. In the Lund string model, which is used in the event generator PYTHIA [80], the colour field between colour charges is approximated by a string between the charges, with an energy that is proportional to the length of the string. This string can break through the production of quark-antiquark pairs from the string energy. In a hadronisation event, the string keeps expanding and breaking until all pieces have small enough energy to be identified with baryons and mesons.

A complete description of a scattering is shown in fig. 3.8 (or almost complete; of course there are further complications which I haven’t discussed, such as remnant treatment and multiple interactions). In practise, the only way to perform simulations of complete events is by using Monte Carlo event generators, which can simulate all these aspects of an event. The two most widely used general-purpose event generators, in which all the aspects discussed here are implemented, are PYTHIA [80] and HERWIG [92]. The final state of an event from these generators includes only long-lived or stable hadrons, leptons and photons, which can then be put through a detector simulation, in order to compare predictions with experimental data.

3.3.2 Parameterisations of total cross-sections

Perturbative QCD does a very good job predicting the rate and phase space distributions of events which involve only a single parton. Examples are deep inelastic scattering events, where a high-energy electron or muon interacts

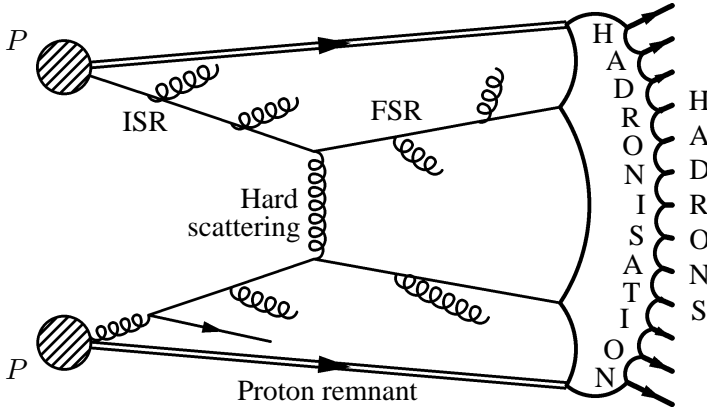


Figure 3.8: A complete simulation of a proton-proton scattering event. Partons from the two protons suffer initial-state radiation and go through a hard scattering. The outgoing partons radiate further (final-state radiation), and finally hadronise to produce the final-state hadrons.

with a quark in the proton, and jet events in hadron-hadron collisions, where two partons have interacted with a large momentum transfer. In the bulk of hadron-hadron collisions however, the situation is even more complicated. The composite hadrons can interact as a whole, without any large momentum transfer in single parton-parton interactions. Therefore perturbative QCD cannot predict properties for total cross-sections. As will be seen in the next section, this is true for electron-hadron interactions at low momentum transfer as well, due to the hadronic nature of the photon.

Even before the advent of QCD, people started to investigate the analytic properties of the scattering matrix S at a very general level. This included the crossing symmetries of Mandelstam [93], which relates the scattering amplitude of the process $a + b \rightarrow c + d$ to the processes $a + \bar{c} \rightarrow d + \bar{b}$ and $a + \bar{d} \rightarrow c + \bar{b}$, as well as a treatment of resonances and the asymptotic behaviour of scattering amplitudes. This so-called Regge pole formalism is quite successful in giving relations between different scattering amplitudes, predicting the masses of higher-spin resonances, and, not the least, in predicting the behaviour of total cross-sections [94].

One common parameterisation of total cross-sections in hadron-hadron collisions, based on Regge theory, is due to Donnachie and Landshoff [95]:

$$\sigma^{\text{tot}} = X s^\epsilon + Y s^{-\eta} \quad (3.38)$$

Here the Mandelstam variable $s = E_{\text{CM}}^2$ is the squared total energy in the

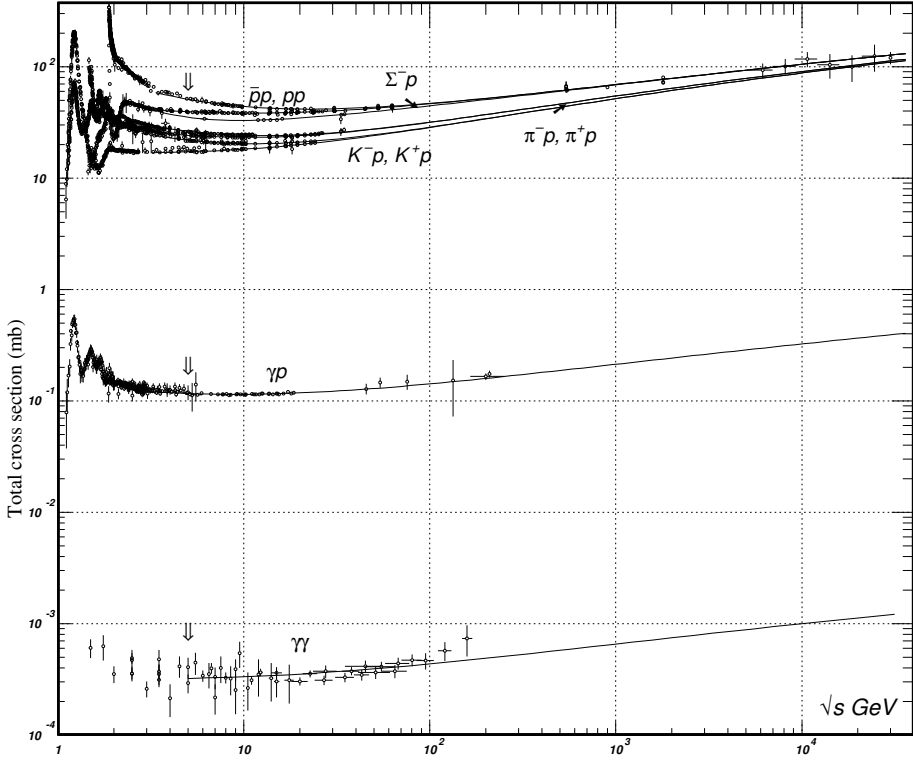


Figure 3.9: The energy dependence of the total cross-section for hadrons and photons, from [14]. The similarity of the behaviour of photons to that of hadrons indicate clearly the hadronic nature of the photon, which can be explained by fluctuation to off-shell vector mesons.

center-of-momentum system of the scattering. The first term corresponds to scattering with exchange of vacuum quantum numbers, a so-called *pomeron*. The second term is called a *reggeon*, and corresponds to the effective exchange of a meson ρ, ω, f, a . The parameters $\epsilon \approx 0.08$ and $\eta \approx 0.45$ are universal constants (or very slowly varying with energy), such that the only difference between different hadrons are in the couplings X and Y . At large energies, $s^{-\eta}$ falls off and leaves the universal total cross-section behaviour

$$\sigma^{\text{tot}} \propto s^{\epsilon} \text{ for } s \rightarrow \infty \quad (3.39)$$

This universal asymptotic behaviour can be seen in the fits to total hadron-hadron cross-section data in the upper part of fig. 3.9.

3.3.3 The hadronic photon

An interesting fact is that the same hadronic cross-section behaviour found in hadron-hadron collisions is also exhibited in photon-proton and even photon-photon scattering (see the lower part of fig. 3.9). This might seem surprising, since the behaviour of the photon in quantum electrodynamics is very different from this hadronic behaviour. However, the phenomenon is readily understood in terms of quantum mechanical fluctuations. In quantum mechanics, a certain state always has a probability to fluctuate into every other state which is allowed by quantum number conservation. The fluctuation probability is given by the coupling and the energy difference (see *e.g.* [96]). Now, the vector mesons ρ^0 , ω , ϕ , J/ψ etc. have the same quantum numbers as the photon ($J^{PC} = 1^{--}$), so we should expect the photon to fluctuate into vector meson states. This hypothesis is called the *vector meson dominance model* (VDM), see [97] for a review. The photon state can then be written as a superposition of a point-like photon $|\gamma_0\rangle$ and a sum of hadronic (vector meson) states $|V\rangle$:

$$|\gamma\rangle = \sqrt{Z} |\gamma_0\rangle + \sum_V \frac{e}{f_V} |V\rangle \quad (3.40)$$

where Z ensures the correct normalisation of the state.

Note the small coupling $\mathcal{O}(\sqrt{4\pi\alpha_{em}})$, which means that it is only a relatively small part of the photon wave function which is hadronic. However, the interaction probability with a hadronic target is much larger for the hadronic components than for the point-like photon, so that the photon-hadron cross-section is dominated by the vector meson interactions. It is possible to estimate the coupling between the photon and the vector meson using the probability (branching ratio) for the vector meson to decay into a pair l^+l^- of charged leptons, or the production probability for the vector meson in e^+e^- collisions (fig. 3.10a).

The interaction between a photon and a target hadron can then be described as the factorisation of two processes: First a fluctuation of the photon into a vector meson V , and then an interaction between the vector meson and the target hadron H (see fig. 3.10b):

$$\sigma_{\gamma H}^{\text{VDM}} = \sum_{V=\rho,\omega,\phi} \frac{e^2}{f_V^2} \left(\frac{m_V^2}{Q^2 + m_V^2} \right)^2 \sigma_{VH} \quad (3.41)$$

where $Q^2 = -k^2$ is the virtuality of the photon with four-momentum k , and the propagator of the vector meson ($1/(Q^2 + m_V^2)$) has been taken into account. The cross-section σ_{VH} can be parameterised using the Regge approach described in the previous section.

However, there is no reason why the photon wave function should be ex-

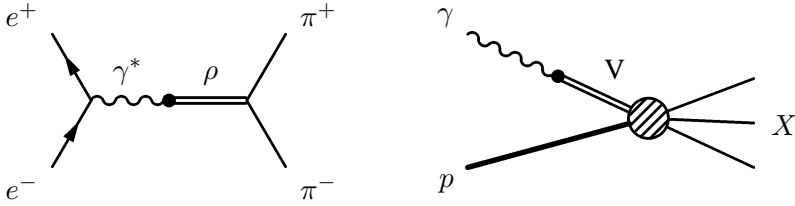


Figure 3.10: (a) Vector meson production in e^+e^- annihilation. The virtual photon couples to a vector meson which is detected through its decay (here the ρ meson decaying to $\pi^+\pi^-$ is taken as an example). (b) The interaction between a photon and a hadron (here a proton), in which the photon first fluctuates into a vector meson. The vector meson interacts with the target hadron with a typically hadronic cross-section, resulting in a hadronic final-state X .

hausted by these discrete, low-lying vector meson states. It is possible to extend this basic VDM cross-section with a continuum of higher-mass hadronic states (see [98, 97]):

$$\sigma_{\gamma H} = \sigma_{\gamma H}^{\text{VDM}} + \sigma_{\gamma H}^{\text{cont}} \quad (3.42)$$

where (in the so-called diagonal approximation)

$$\sigma_{\gamma H}^{\text{cont}} = \int_{m_0^2}^{\infty} \frac{\rho(s, m^2)}{(Q^2 + m^2)^2} dm^2 \quad (3.43)$$

The spectral function $\rho(s, m^2)$ can be estimated using the cross-section for $e^+e^- \rightarrow$ hadrons and some parameterisation for the hadronic cross-section, such as eq. (3.38).

This formalism gives a good description of photon-hadron interactions at low Q^2 (and can be extended to work for larger Q^2 , see *e.g.* [99]). As we show in paper I, it also gives a good description of the proton structure function F_2 (see below) in the low- Q^2 , low- x region. At larger $Q^2 \gtrsim 4 \text{ GeV}^2$, interactions are well described by the DIS (deep inelastic scattering) picture, where the point-like photon interacts with a parton in the proton, as described in section 3.2 above.

3.4 QCD and partons in the search for new physics

As mentioned in chapter 2, the Standard Model is extremely successful. All precision measurements at LEP, Tevatron and other accelerators agree well with the Standard Model, and there are yet no conclusive experimental deviations from it. Detailed studies of the experimental limits on new physics show

that new interactions must be suppressed by particle masses around 2–10 TeV (assuming couplings of $\mathcal{O}(1)$) [29]. In view of the fact that the Standard Model is unsuitable to be the correct description of the world already at scales above 1 TeV because of the problems discussed in sec. 2.2, this means that the experimental resolution should already be high enough to be able to distinguish effects of new physics.

Therefore, particle physicists all over the world are searching vigorously for experimental deviations from the Standard Model. And indeed, recent history has shown several examples of deviations from Standard Model predictions. However, although these have at first been attributed to new physics, they have so far been found to be explained by means of some aspect of Standard Model physics, which was previously not properly understood. One such example is the excess of jets at large transverse energy at the Tevatron, mentioned in sec. 3.2.5 above, which could be explained by a surprisingly large gluon density at large x in the proton. Another example, which is still controversial, is the NuTeV anomaly reported in 2001, which might also turn out to be explained by a better understanding of parton density functions.

3.4.1 The NuTeV anomaly

I will treat the NuTeV anomaly in some detail since one of the papers in this thesis (paper II) focuses on a possible explanation for it. The NuTeV experiment at Fermilab near Chicago, USA, measured neutrino and antineutrino interactions with a very large iron target [100]. Since they had the possibility to alternate between high-purity ν_μ and $\bar{\nu}_\mu$ beams, they could measure cross-sections for neutrinos and antineutrinos separately. This enabled quite precise measurements of several Standard Model parameters, most notably the electroweak mixing angle $\sin^2 \theta_W$ (see chapter 2, sec. 2.1.4). They measured this parameter by means of a ratio of neutral current to charged current cross-sections, inspired by the Paschos-Wolfenstein ratio [101]

$$R_{\text{PW}} \equiv \frac{\sigma(\nu_\mu N \rightarrow \nu_\mu X) - \sigma(\bar{\nu}_\mu N \rightarrow \bar{\nu}_\mu X)}{\sigma(\nu_\mu N \rightarrow \mu^- X) - \sigma(\bar{\nu}_\mu N \rightarrow \mu^+ X)} = g_L^2 - g_R^2 \equiv \frac{1}{2} - \sin^2 \theta_W \quad (3.44)$$

which is true for an isoscalar target. The value found by NuTeV was [102]

$$\sin^2 \theta_W^{\text{NuTeV}} = 0.2277 \pm 0.0013(\text{stat.}) \pm 0.0009(\text{syst}) \quad (3.45)$$

which is 3σ above the Standard Model fit $\sin^2 \theta_W = 0.22272 \pm 0.00036$ (see chapter 2, eq. (2.33)). This is the only precision measurement of this quantity by a neutrino experiment, which means that new physics affecting the weak interaction could very well influence this measurement without contributing

to other kinds of measurements of $\sin^2 \theta_W$. Therefore the result caused quite some excitement, and a number of new physics explanations were suggested, such as leptoquarks, extra heavy vector bosons and non-universality in gauge couplings to leptons and quarks [103]. However, most new physics possibilities could be ruled out, at least if they were to explain the full anomaly [104].

There are also several effects within the Standard Model that can explain (parts of) the anomaly [104], and which were not accounted for in the extraction of the value (3.45). The most important have to do with parton densities. The reason is that neutrinos and antineutrinos have different charged-current interactions with quarks due to electric charge conservation: A muon-neutrino can change into a (negative) muon by emitting a W^+ , while an antineutrino can only change into a positive antimuon, and hence only emit a W^- . Charge conservation then implies that a neutrino can only interact with down-type quarks and up-type antiquarks (*cf.* fig. 3.7a), and vice versa for the antineutrino. This means that if there are differences between *e.g.* the distributions of s and \bar{s} in nucleons, or between the u in the proton and the d in the neutron, this would have an impact on the quantity R_{PW} and therefore affect the extraction of $\sin^2 \theta_W$.

For the strange sea, the *number integral* $\int_0^1 (s(x) - \bar{s}(x))dx = 0$, but there is no conservation law that forbids the *momentum integral* $\int_0^1 (xs(x) - x\bar{s}(x))dx \neq 0$. A positive strange quark momentum asymmetry $\int_0^1 (xs(x) - x\bar{s}(x)) > 0$ in the nucleons would give a smaller value for R_{PW} , resulting in an artificially large $\sin^2 \theta_W$. Such an asymmetry is precisely what we predict in the papers II and III based on our physically motivated model for parton densities. According to our model, the effect is large enough to explain about 1σ of the discrepancy. Recently, a new analysis of NuTeV di-muon data [105], from which it is possible to extract the s and \bar{s} distributions separately (see fig. 3.7a), has revealed that their data shows an s - \bar{s} -asymmetry similar in magnitude to what we predicted.

The other effect mentioned above that would influence the extraction of $\sin^2 \theta_W$ from R_{PW} would be isospin breaking, *i.e.* an excess of d quarks in the neutron relative to u quarks on the proton, $\int_0^1 (xu^p(x) - xd^n(x))dx < 0$. Recently, an estimate has been made of the isospin breaking induced by photon radiation in the evolution of parton densities [106], similarly to the gluon radiation described in sec. 3.2.2 and 3.2.3. This effect is very small due to the smallness of the electromagnetic coupling $\alpha_{em} \approx 1/137$, but large enough, and with the right sign, to reduce the NuTeV anomaly by another 1σ . However, both these explanations might need more experimental support before the issue can be considered settled.

These examples show that, historically, signals for new physics have turned out rather to be signals that we need to improve our understanding of Standard Model physics. But let us now move on to the future, and the Large Hadron

Collider.

3.4.2 QCD and new physics at the LHC

All the scenarios for solving the problems with the electroweak symmetry breaking that I discussed in chapter 2, sec. 2.3, imply the existence of new particles with masses below or around 1 TeV. At present, the global high energy physics community has joined in the effort to build a huge proton-proton collider, the Large Hadron Collider (LHC) at CERN [107]. This collider, with the experiments ATLAS, CMS, ALICE, LHC-B and TOTEM, is expected to start operation during 2007. Thanks to the large center-of-momentum energy (14 TeV) and luminosity of the LHC, it is expected to be able to probe at least parts of the new particle spectra for all those scenarios (see eg. [108]).

However, the LHC is a proton-proton collider. This means that QCD plays a very important role in the extraction of signals for new physics, for at least two reasons: First, in hadron collisions, there is a large background in terms of Standard Model particles and jets, especially when the collision energy is large. Second, the new particles will be produced from quarks and gluons (mainly through gluon-gluon fusion) and usually together with extra quarks and gluons, causing the predictions for production rates and distributions to be sensitive to QCD effects. Both these effects imply that a very good knowledge and understanding of QCD and QCD effects is vital for success in the search for new physics at the LHC.

I will now discuss a few topics that connect to my own research.

Uncertainties from parton densities

The most interesting processes at the LHC will involve production of heavy particles. This means that the QCD evolution scale (factorisation scale) will be large. Still, the large total center-of-momentum energy available means that the momentum fractions x taken by the partons involved can be relatively small, even in production of particles as heavy as several hundred GeV. Due to the DGLAP evolution, these two effects result in a huge dominance of the gluon density over all quark densities. Therefore, a large number of interesting processes are initiated by two gluons fusing to produce the new heavy particles.

On the other hand, the main sources of experimental knowledge of parton distributions available today are HERA, an electron-proton collider at DESY in Hamburg, Germany, and the proton-antiproton collider Tevatron at Fermilab near Chicago, USA. The experiments at HERA are of DIS type (described in sec. 3.2.1), which means that the hard interaction is mediated by photon exchange. There, only quark and antiquark parton densities can be directly probed, while the gluon density is mainly inferred from the DGLAP evolu-

tion and higher-order photon-gluon fusion processes such as $\gamma g \rightarrow c\bar{c}$. At the Tevatron, high-energy collisions between protons and antiprotons are investigated. At the center-of-momentum energy of the Tevatron (1.96 TeV), the valence quark distributions still dominate at the relatively large x where the most interesting processes (W^\pm production and $t\bar{t}$ production) take place. Also, a valence quark from the proton and a valence antiquark from the antiproton can annihilate to produce new particles, while at the LHC a valence quark must annihilate with an antiquark from the low- x quark sea of the other proton. All this means that the extrapolation of parton densities from presently running experiments to the LHC is difficult, especially for the very important gluon density.

The two leading groups working with the extraction of parton density functions from experimental data, MRST [109] and CTEQ [83], have both produced different sets of parton density functions with different values of the fitting parameters, which reflect the effect of experimental uncertainties on the extraction of parton density parameterisations. In order to find the uncertainty due to parton density functions in a given observable, *e.g.* the production rate of some particle, the observable should be calculated using all the parton density sets. The spread in the results is then interpreted as the uncertainty in the calculated observable. Such investigations show that the cross-section for jet production at very large transverse energies ~ 1 TeV has an uncertainty close to a factor 2 [110].

Furthermore, the two groups have made estimates of the theoretical uncertainties connected to different parameterisations of the starting distributions, and also on the dependence on which data sets are included in the fits. If a fit is to be reliable, it should be relatively insensitive to variations in these details. Both the groups have made special case studies of W^\pm production at the LHC, which is a very important process since it may serve as a luminosity monitor. However, the situation at present is quite confused; the MRST group claims [111] that they get a theoretical uncertainty of the order 20% using next-to-leading order (NLO) calculations. CTEQ however, when they did a similar variation, found a very small theoretical uncertainty of the order few per cent at NLO [112]. This issue is not fully resolved at the time of writing.

Furthermore, there might be uncertainties related to so-called higher-twist effects at low Q^2 . One such effect could be the contribution from VDM-like photon-proton interactions, which might be non-negligible up to $Q^2 \sim \text{few GeV}^2$, as we argue in paper I. In that case, the extraction of the gluon and sea quark densities at low x might be erroneously compensating for such a non-partonic component of the cross-section at low Q^2 , which would affect the parton densities at higher Q^2 via DGLAP evolution. In any case, the uncertainty factor from the gluon density function in the production of heavy particles certainly should be taken seriously.

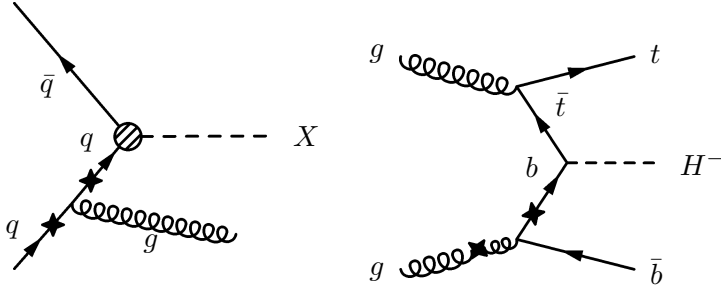


Figure 3.11: (a) Diagram describing the two processes $ab \rightarrow X$ and $ab' \rightarrow cX$ in the case $a = \bar{q}$, $b = b' = q$ and $c = g$. X can be any massive system, e.g. a Higgs boson or a lepton pair with large invariant mass. The crosses on the incoming quark line symbolise the two different factorisation points corresponding to the two processes. If we make the factorisation before the gluon emission, the gluon emission is considered to be a part of the hard scattering, meaning that we need to calculate the full matrix element of the $q\bar{q} \rightarrow gX$ process. If we instead make the factorisation after the gluon emission, the hard process is considered to be $q\bar{q} \rightarrow X$, while the gluon emission is a part of the initial state parton shower described by the DGLAP equations. (b) A similar diagram for the special case of charged Higgs production in association with top and bottom quarks, considered in paper VI.

Higher order calculations and matching with parton showers

Another difficulty in the production of heavy particles at the LHC is the matching of higher-order matrix element calculations with parton showers mentioned in sec. 3.2.4. I will here concentrate on initial state parton showers, but the problems with, and treatment of, final-state parton showers are similar. I will also only discuss tree-level processes.

In a partonic scattering process where two quarks or gluons a and b interact to produce a massive system X , the DGLAP equation resums the logarithmically enhanced parton emissions from the interacting partons. For such a production process, these parton emissions give the dominating contribution to the total cross-section, which is therefore well described by this formalism. However, it does not give a good description of jets emitted with large transverse momenta. This is because the DGLAP equations only takes into account the soft and collinear emissions, as discussed in sec. 3.2.3.

If we are interested in the process where one of the emitted partons gives rise to a jet with large transverse momentum, we need to calculate the full matrix element for this process $ab' \rightarrow Xc$ (see fig. 3.11a), based on its Feynman diagrams. This calculation is one order higher in α_s since there is an extra strong interaction vertex. It takes into account interference between different diagrams, and gives a result which is valid for large values of the transverse

momentum of the outgoing parton c . However, it does not take into account the logarithmically enhanced collinear terms which are resummed by the DGLAP equations. This means that the two descriptions, the parton emission via the DGLAP parton shower and the exact matrix element, can be viewed as two different approximations of the same basic process (see fig. 3.11a). If we want a description which is as good as possible in the whole phase space of the outgoing parton c , we should take both these approximations into account.

However, if we naively sum the two processes, we get double-counting of emissions with small transverse momenta. This is because the calculation of the exact matrix element of the emission process already includes the leading order logarithmically enhanced emission (the emission corresponding to eq. (3.21) in the case of DIS). For small transverse momentum of the outgoing parton c , the cross-section for $ab' \rightarrow Xc$ can be written as a convolution of the probability to have a parton b' splitting to a bc pair $\mathcal{P}(b' \rightarrow bc)$ and the cross-section $\sigma_{ab \rightarrow X}$ for ab fusion:

$$\sigma_{ab' \rightarrow Xc} = \mathcal{P}(b' \rightarrow bc) \otimes \sigma_{ab \rightarrow X} + \text{finite corrections} \quad (3.46)$$

The “finite corrections” are the parts of the cross-section that are not logarithmically enhanced, *cf.* the functions $C_{q,g}(x)$ in eq. (3.32). The first term on the right-hand side of eq. (3.46) is then double-counted, since it is present in both the matrix element calculation and the parton shower. For details of this convolution, I refer to paper VI where the case $gb \rightarrow H^\pm t$ is treated.

There are different solutions to the matching of the matrix element and parton shower descriptions. One approach, which is used for some simple processes in the event generator PYTHIA [80], is to use only the parton showers, but make corrections to the hardest emission in the shower in such a way as to mimic the behaviour of the hard emission from the matrix element calculation. This is done by raising the maximum virtuality to ensure that all possible emissions are produced, and then applying a correction factor to the probability for emission. In this approach, the total cross-section is still given by the lowest-order process (here $ab \rightarrow X$), and only the branching with the largest t is corrected. A more recent development, which is constructed to work for any number of outgoing parton jets, is the so-called CKKW algorithm, see [113].

In paper VI, we have considered the special case of charged Higgs boson production at the LHC (or Tevatron) together with top and bottom quarks. The coupling of charged Higgs boson to quarks is proportional to their mass. Therefore the coupling to the light quarks is negligible in comparison to the coupling to top and bottom quarks. The main production process is $bg \rightarrow H^- t$ ($\bar{b}g \rightarrow H^+ \bar{t}$), where the b quark is treated as a parton in the proton. Assuming that there are no b quarks in the proton at the starting scale of the DGLAP evolution, the b quark must originate in a gluon splitting somewhere in the

evolution chain (see fig. 3.11b), and there must be a corresponding \bar{b} in the final state. We thus have a situation of the kind described above, where the best description of the outgoing \bar{b} is given by the matrix element of the $gg \rightarrow H^- t \bar{b}$ process for large transverse momenta, and by parton showers from the $g\bar{b} \rightarrow H^- t$ for small transverse momenta. Our solution to the double-counting problem is to subtract the double-counted component $\mathcal{P}(g \rightarrow b\bar{b}) \otimes \sigma_{g\bar{b} \rightarrow H^- t}$ from the sum of the processes on the fully differential cross-section level. Our treatment allows us to take into account constraints in the kinematics of the outgoing particles. It also gives a method to estimate a reasonable factorisation scale for the process.

Factorisation scale dependence

The factorisation scale, which was introduced in sec. 3.2.2, is the scale at which the parton densities are evaluated as they are convoluted with the matrix element of a hard scattering process. If we were able to calculate the cross-section for the process to all orders in perturbation theory, *i.e.* sum up all terms in the expansion in α_s , there would be no factorisation scale dependence, and the scale would be completely arbitrary. Unfortunately, in real life we can only calculate the first few terms in the expansion, and we therefore get a residual dependence on the scale chosen. Through the DGLAP equations, the magnitude of the parton densities depend on the value of the factorisation scale. This dependence can be quite sizable, especially for the gluon density, which means that gluon initiated processes are extra sensitive to the choice of factorisation scale. Therefore it is important to find good arguments for the choice of factorisation scale. Similar considerations apply to the *renormalisation scale* introduced in sec. 3.1.1, *i.e.* the scale where the strong coupling is evaluated. For a discussion of the choice of renormalisation scale, see *e.g.* [114].

The factorisation (and renormalisation) scale dependence gets smaller for each higher order term we include in the calculation. This can be seen in the case of deep inelastic scattering for the proton structure function F_2 in eq. (3.18) and (3.24)-(3.25): In the leading order expression for F_2 , eq. (3.18), there is no explicit factorisation scale dependence, which means that the factorisation scale dependence of the parton distributions is directly transferred to F_2 . The next-to-leading order (NLO) expression, eq. (3.25), has an explicit factorisation scale dependence which exactly cancels the first logarithmic dependence in the parton densities, as seen in eq. (3.24). Therefore the full NLO calculation is left with only the dependence from higher powers of the logarithm and α_s , and the scale dependence is reduced relative to the leading order calculation.

Since the leading order expression completely lacks explicit scale dependence, it doesn't by itself give any clue to which scale is an appropriate choice. This means that it is in principle necessary to calculate the NLO expression

to get an idea of which scale might be suitable for the process in question. In the case of deep inelastic scattering, the NLO calculation suggested that Q^2 , the virtuality of the photon, was a suitable choice. This was because with this choice of scale, all the large logarithms of higher order terms reside in the evolution of the parton densities, ensuring that the corrections from higher order calculations are small.

However, deep inelastic scattering, where only the scattered lepton is observed, is a relatively uncomplicated process, since it only involves one large mass scale, the virtuality of the exchanged photon. In more complicated cases with several large scales, such as multiple particle production in hadron-hadron collisions, the choice is not as simple. In general, the factorisation scale should be connected with the scales in the process, such as masses or transverse momenta of the outgoing particles. Still, in order to find which combination of scales is the best choice, and how they should be weighted, it is necessary to go to higher order calculations.

In our paper VI, we suggest a way to determine the appropriate factorisation scale in the case of the charged Higgs production process $gb \rightarrow H^\pm t$ discussed above, which can be generalised to other processes as well. This method gives similar results as methods suggested by other authors (see references in paper VI), but is based on different arguments. In our method, we compare the momentum distribution from the matrix element of the process $gg \rightarrow H^\pm tb$ with the leading QCD emission term of the parton shower of the $gb \rightarrow H^\pm t$. This latter term gives precisely the double-counting between the matrix element and the parton shower, as discussed in connection with eq. (3.46) above. Now, in order to have a physically meaningful picture, this double-counting component should be a good approximation to the collinear part of the higher order term. Since the magnitude of the double-counting component depends directly on the factorisation scale, we get a rather restricted allowed region for the factorisation scale by demanding that the double-counting component should not be larger than the matrix element for $gg \rightarrow tbH^\pm$ anywhere in the phase space, but also not much smaller in the collinear region.

An advantage with this method is that it is not necessary to calculate the full NLO cross-section for the $gb \rightarrow H^\pm t$ process, since only the tree-level matrix element for the process with an extra outgoing parton in the hard scattering is needed to find a suitable factorisation scale.

4. Summary of papers

Paper I: *Interpretation of electron-proton scattering at low Q^2*

We apply the generalised vector meson dominance model (GVDM) to electron-proton scattering at low momentum transfer, and show that it gives a very good description of the proton structure function F_2 at low x and $Q^2 \leq 0.65 \text{ GeV}^2$. We suggest a combination of the GVDM description at low Q^2 with the standard parton distribution formalism at larger Q^2 , and show that this can give a description of F_2 which is valid for all Q^2 .

Paper II: *Strange quark asymmetry in the nucleon and the NuTeV anomaly*

We make a dedicated study of the effect on the NuTeV anomaly from the momentum distribution asymmetry between strange and anti-strange quarks in the nucleon sea, as predicted by the model for parton distributions in hadrons described in detail in paper III. The asymmetry in the strange sea distributions is due to fluctuations into baryon-meson pairs, *e.g.* ΛK , where the strange quark resides in the baryon and the anti-strange quark in the meson. This effect is found to be large enough to reduce the NuTeV anomaly to a level where there is no longer any strong hint for physics beyond the Standard Model.

Paper III: *Quark asymmetries in the proton from a model for parton densities*

In this paper we give a detailed presentation of the development of a model for parton densities in nucleons. The model is based on quantum fluctuations of the momenta of partons in hadrons, and fluctuations of the nucleon into baryon-meson pairs. This model describes structure function data, and is shown to reproduce important quark asymmetries in the proton, such as the difference between anti-up and anti-down sea quarks and the shape difference between up and down valence quarks. Another consequence of the model is an asymmetry between the strange and anti-strange sea quarks, which is of interest in connection with the NuTeV anomaly.

Paper IV: *Quark asymmetries and intrinsic charm in nucleons*

Here we give a short review of our model for parton distributions in hadrons, described in detail in paper III. We also make a special study of the possibility

of intrinsic charm in the proton, due to fluctuations of nucleons into charmed baryon-meson pairs, *e.g.* $\Lambda_C \bar{D}$. We show that the charm quark distribution from such fluctuations can explain the excess in EMC charm structure function data at large x .

Paper V: *The $p\bar{p} \rightarrow tbH^\pm$ process at the Tevatron in HERWIG and PYTHIA simulations*

We compare the predictions for charged Higgs boson production at the Tevatron by PYTHIA and HERWIG. We also make a comparison, for charged Higgs boson masses $m_{H^\pm} < m_t - m_b$, between the (approximate) production channel $gg(q\bar{q}) \rightarrow t\bar{t}$ with $t \rightarrow H^+b$ ($\bar{t} \rightarrow H^-\bar{b}$), and the full process $gg(q\bar{q}) \rightarrow H^-t\bar{b}$ ($H^+t\bar{b}$). For this paper, I implemented the $gg(q\bar{q}) \rightarrow H^\pm tb$ processes into PYTHIA.

Paper VI: *Improved description of charged Higgs boson production at hadron colliders*

We present a new method for matching the two dominating contributions for production of charged Higgs bosons at hadron colliders. If naively summed, the processes, $gb \rightarrow H^\pm t$ and $gg \rightarrow H^\pm tb$, give double-counting in the region of collinear momenta of the b quark. Our matching procedure corrects for this double-counting, and gives a transition between the collinear region, which is best described by the $gb \rightarrow H^\pm t$ process, and the large-transverse momentum region, described by the process $gg \rightarrow H^\pm tb$. This is found to be necessary when the outgoing b -quark is tagged. We show that our matching procedure works at a fully differential level and gives smooth differential cross-sections in all kinematical variables. Our matching also allows us to give an argument for the optimal choice of factorisation scale for the process $gb \rightarrow H^\pm t$, by comparing the double-counted component with the $gg \rightarrow H^\pm tb$ term.

Paper VII: *MATCHIG: A program for matching charged Higgs boson production at hadron colliders*

This paper is a manual on how to use the Monte Carlo computer routine MATCHIG. This is an implementation of our algorithm for matching the charged Higgs boson production processes $gb \rightarrow tH^\pm$ and $gg \rightarrow tbH^\pm$, described in paper VI. The event generator, which corrects for the double-counting between the two processes using negative-weight events, is implemented as an external process to PYTHIA. Using this process together with the internally implemented production processes gives a generation of matched events at a fully differential level, as well as the correctly matched integrated cross-section.

5. Conclusions and outlook

In this thesis, I have emphasised the understanding of the strong interaction and proton structure as key ingredients in the description of the fundamental components of the world. The proton is interesting, not only in its own right (after all, more than 99% of the mass of our bodies are in the form of protons and neutrons), but it is also instrumental in the search for new physics. Both the Tevatron and the LHC are proton colliders, which means that a precise understanding of collisions involving protons is necessary to be able to discriminate between Standard Model physics and signatures for new physics beyond the Standard Model.

The research I have presented here is divided into two main projects. Papers I-IV are concerned with the internal structure of the proton, with its interactions at low momentum transfer and how the quarks are distributed. Papers V-VII have a quite different focus: production of new heavy particles at hadron colliders. However, both these projects are connected to the interplay between the understanding of the proton and the search for new physics.

Parton densities are essential to the interpretation of possible signals for physics beyond the Standard Model. This has been shown recently in the case of the so-called NuTeV anomaly, which could be interpreted as a deviation from the predictions of the Standard Model, suggesting the influence of new physics. It is now very probable that the anomaly can be explained by features in the distributions of quarks in the proton and neutron, which were previously not well understood. At the LHC, parton densities will be an important source of theoretical uncertainty for many processes. Therefore, all efforts to get a better description of parton densities are important.

We have constructed a physical model for the parton densities, which can explain many features found in experimental data. By studying in which aspects the model works and where it fails, we can contribute to the understanding of the physics underlying the parton distributions in hadrons. We have also been able to use the model to make predictions for aspects of the parton densities that have not yet been accurately measured, such as the strange and charm quark distributions of the proton. We are working on extending these predictions and to make comparisons with new sets of experimental data.

Production of heavy particles at the LHC will probably be the main signature for physics beyond the Standard Model in the years to come. It is impor-

tant to minimize the theoretical uncertainties for these production processes, for at least two reasons: One is that, in order to disentangle signals for new physics from the Standard Model background, we must have search strategies that suppress the background. To devise search strategies we need to have an accurate description of such aspects as momentum distributions of the particles in the process and decays of the new particles, as well as for the background processes. Another reason is that once we have found signatures for new physics, we want to be able to discriminate between different models for this new physics, which will demand a very good understanding of the predictions of different models.

So far, my research in this area has concentrated on production of charged Higgs bosons. These particles are predicted by Supersymmetry, one of the most popular ideas for extending the Standard Model. Charged Higgs bosons also appear more generally in any model with two Higgs doublets, so called *two Higgs doublet models*. If such a particle is observed at the Tevatron or LHC, it would be a definite sign of physics beyond the Standard Model, since no charged scalar particle exists in the Standard Model.

We have studied different processes for charged Higgs boson production in association with top and bottom quarks, which is the dominating production mechanism at proton colliders. In order to combine the two dominating processes, we have developed an algorithm to compensate for double-counting when the outgoing b -quark has small transverse momentum, and implemented the algorithm as a Monte Carlo event generation program. This procedure allows for a smooth interpolation between the regions with small and large transverse momenta of the outgoing b -quark, and also gives a method to determine the factorisation scale in the process. A study of the charged Higgs boson production in the ATLAS experiment at the LHC is underway, based on our procedure, using full detector simulation and careful studies of the Standard Model background. Our methods can also be extended to the production of other particles, and work is in progress to apply the methods to the production of neutral Higgs bosons in association with b -quarks, which can be an important production mechanism in two Higgs doublet models.

These are very exciting times to do research in particle physics; we are soon going to reach the frontier when the theories we use today to describe the fundamental particles and interactions in nature will no longer be enough. It might well be that the Large Hadron Collider will be the starting point of a new explosion of particles, similar to the “zoo of hadrons” discovered in the 1960’s. Supersymmetric particles, Higgs particles, Kaluza-Klein particles, new gauge interactions; they are all predicted by theories for new physics, but we have no idea which, if any, of these theories is realised in nature. Perhaps we will find something completely unforeseen, which would be the most exciting of all.

6. Summary in Swedish – Populärvetenskaplig sammanfattning

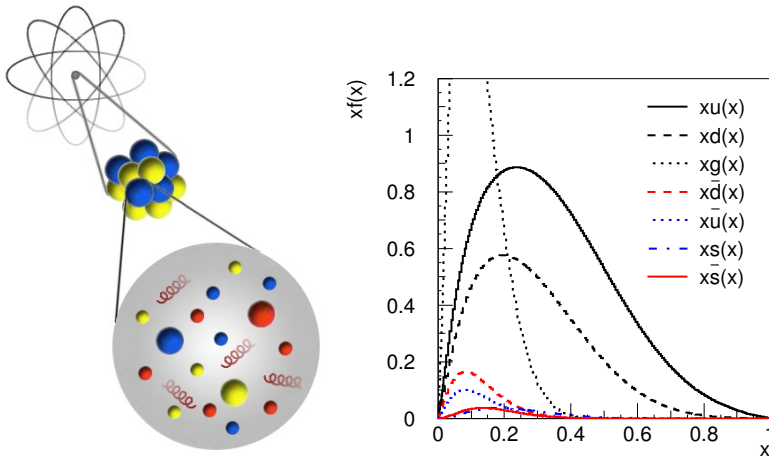
Kvarkfördelningar och produktion av laddade Higgs-bosoner – Studier av protonens struktur och ny fysik

Vetenskapen om materiens grundläggande beståndsdelar har under de senaste hundra åren gjort fantastiska framsteg. Inte nog med att vi nu vet att allt är uppbyggt av atomer med en radie på ungefär 1/10 000 000 millimeter; atomerna består i sin tur av en tung, positivt laddad kärna som är ännu mycket mindre (dess diameter är c:a 1/100 000 av diametern hos en atom) omgiven av lätta, negativt laddade elektroner. Vi har lyckats tränga in även atomkärnan, och funnit att den består av kärnpartiklar: protoner, som är positivt laddade med exakt motsatt laddning mot elektronen, och neutroner, som är oladdade. I epokgörande experiment vid Stanfords linjäraccelerator i slutet av 1960-talet kunde man slutligen visa att även protonerna består av mindre partiklar. I dessa experiment använde man elektroner som accelererats till hastigheter nära ljusets för att försöka sönderdela själva protonen.

Det visade sig att det inte går att dela upp protonen i dess beståndsdelar, men man kunde ändå se att den består av ännu mindre partiklar. Dessa partiklar kom att kallas *kvarkar*, och har en laddning som mäts i tredjedelar av elektronens laddning. Protonen består av två uppkvarkar och en nerkvark, medan neutronen består av en uppkvark och två nerkvarkar. Märkligt nog kan dessa partiklar bara existera "inlåsta" i t.ex. protoner och neutroner. Därför kan man alltså inte i egentlig mening dela en proton och få ut kvarkarna som bygger upp den. Vi vet inte hur små kvarkarna egentligen är, men genom experiment har man kunnat räkna ut att deras diameter i alla fall är mindre än 1/1000 av protonens, och såvitt man vet är såväl kvarkar som elektroner verkligt elementära (alltså odelbara) partiklar.

Kvarkfördelningar inuti protonen

Ett av de två projekt som jag har arbetat med för den här avhandlingen handlar om att försöka förstå hur kvarkarna är fördelade inuti protonen (artiklarna I-IV). Vid DESY-laboratoriet utanför Hamburg kolliderar man protoner och elektroner som accelererats till mycket höga hastigheter. Genom att analysera hur elektronerna sprids efter kollisionen kan man få reda på hur stor del av



Figur 6.1: Till vänster illustreras en proton med dess beståndsdelar: tre *valenskvarkar* som bestämmer protonens laddning, en mängd *gluoner*, som är bärare av den starka kraften och binder samman kvarkarna (visas som spiralfjädrar), och dessutom *sjökvarkar*, kvarkar och antikvarkar som existerar som kvantfluktuationer i protonen. Till höger ett diagram som visar de olika kvarkarnas och gluonernas energifördelningar i protonen, enligt den modell vi utvecklat (från artikel III). Variabeln x står för andel av protonens energi. Figurer av författaren.

protonens rörelseenergi som de olika typerna av kvarkar har. Kunskap om dessa kvarkfördelningar är nödvändig för att man ska kunna förutsäga protoners beteende i framtida kollisionsexperiment. I allmänhet brukar man använda en mer eller mindre godtycklig funktion för kvarkfördelningarna, med vissa parametrar som anpassas till data.

Vi har istället utarbetat en fysikaliskt motiverad modell för dessa kvarkfördelningar, se figur 6.1. Modellen bygger på kvantfluktuationer i protonen, och kan hjälpa oss att förstå hur det kommer sig att vissa kvarkfördelningar uppvisar karakteristiska asymmetrier. Vi har bl.a. använt modellen för att förutsäga en asymmetri i protonen mellan s.k. särkvarkar (som är kusiner till nerkvarkarna) och deras antipartiklar. Den asymmetrin är särskilt intressant för att den kan hjälpa till att förklara en avvikelse från vad som förutsagts inom Standardmodellen, som mättes i neutrinoexperimentet NuTeV vid Fermilab utanför Chicago.

Standardmodellen

Standardmodellen är vår hittills bästa teori för materiens minsta beståndsdelar. Det är en mycket framgångsrik teori, som lyckats beskriva alla elementarpartiklar vi känner till från experiment. Dessa partiklar är dels kvarkar, som är av sex sorter, *upp-*, *ner-*, *sär-*, *charm-*, *botten-* och *toppkvark*, och dels

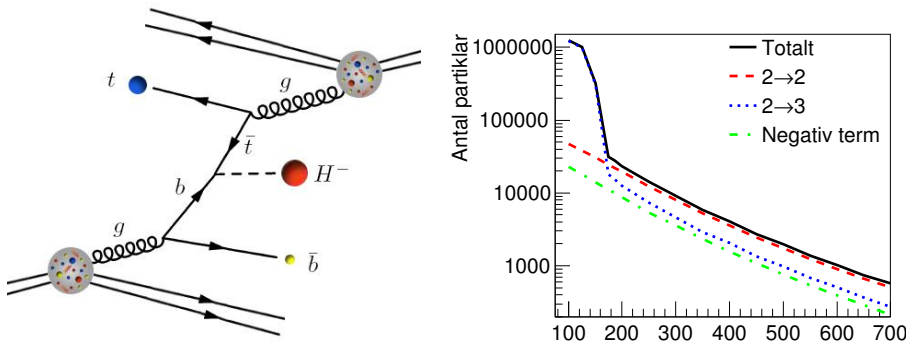
leptoner, som också är av sex olika slag: *elektron*, *myon* och *tauon* samt en *neutrino* för var och en av dessa tre. Standardmodellen beskriver också de krafter, eller *växelverknningar*, som verkar mellan dessa partiklar, och som förmedlas mellan partiklarna med hjälp av s.k. *bosoner*. De krafter vi känner till är den elektromagnetiska kraften, den svaga och den starka kraften samt gravitationen. Gravitationen har ännu inte kunnat beskrivas i samma formalism som de andra krafterna, och är därför egentligen inte en del av Standardmodellen. Detta är emellertid inget problem för partikelfysiken eftersom gravitationen är oerhört mycket svagare än de andra krafterna när det handlar om så små och lätta partiklar.

Higgspartikeln ger massa

En intressant aspekt hos Standardmodellen är att alla fundamentala partiklar enligt denna teori egentligen är masslösa. För att partiklarna ska få massa krävs någon speciell mekanism. Det enklaste sättet att åstadkomma detta, och det sätt som används i Standardmodellen, är att man inför en mycket speciell partikel som kallas för Higgspartikeln. Denna partikel har egenskapen att den förändrar vakuum så att andra partiklar får massa då de passerar genom det. Det finns dock problem med denna bild. Ett ganska uppenbart sådant är att vi ännu inte lyckats hitta Higgspartikeln, trots intensivt letande såväl vid LEP-acceleratorn vid CERN-laboratoriet utanför Genève som vid Fermilabs accelerator Tevatron. Standardmodellen kan inte förutsäga Higgspartikelns massa, bara att den måste vara under en viss övre gräns på ungefär 700 gånger massan hos en proton. Dock kan man göra anpassningar av alla parametrar i Standardmodellen och på så sätt få fram vilken massa Higgspartikeln borde ha för att teorin ska beskriva experimentresultat, och då får man mycket lägre värden för massan. Bäst anpassning till de experimentella data får man om Higgspartikeln har en massa som är så låg att man redan borde ha sett den vid LEP.

Utvidningar av Standardmodellen

Higgspartikelns massa ställer dock till även andra problem. I Standardmodellen finns nämligen mekanismer som gör att denna massa borde vara lika stor som den s.k. Planckmassan, som är helt ofattbart mycket större än en protonmassa (Planckmassan kan skrivas som en etta med 19 nollor efter, gånger protonmassan). Samtidigt kräver alltså teorin att den är mindre än ungefär 700 gånger protonmassan. Denna motsägelse kan bara lösas om det finns någonting, ytterligare krafter och/eller partiklar, som "skyddar" Higgsmassans låga värde. En teori som förutsäger ett sådant skydd är *supersymmetri*. Supersymmetri innebär en utvidgning av själva rumtidens symmetri. Enligt denna teori borde varje materierpartikel (fermion, d.v.s. kvark eller lepton) ha en motsvarighet som påminner mer om en växelverkanspartikel (en boson), och vice versa. Denna andra partikel, som



Figur 6.2: Till vänster visas produktion av en laddad Higgspartikel tillsammans med en topp- och en botten-kvark i en proton-proton-kollision. Två gluoner från protonerna kolliderar och producerar topp- och bottenkvarkar, som i sin tur producerar en laddad Higgspartikel, medan resterna av protonerna fortsätter framåt. Till höger ett diagram (från artikel VI) över antalet laddade Higgspartiklar som kan komma att produceras vid LHC under första året, som funktion av partikelns massa. De olika kurvorna motsvarar olika produktionsbidrag. Observera att bara en liten andel av dessa partiklar kommer att kunna observeras. Figurer av författaren.

kallas superpartner, borde ha i övrigt identiska egenskaper, inklusive samma massa, som den vanliga partikeln. Så kan det dock inte vara, eftersom vi då redan borde ha sett superpartners till t.ex. elektronen och fotonen. Dock kan man tänka sig att supersymmetrin bara är en ungefärlig symmetri, och de supersymmetriska partiklarna kan då ha massor som är mycket högre än de vanliga partiklarnas massor. För att teorin fortfarande ska åstadkomma det den var tänkt för, nämligen skydda Higgsmassan från att bli för stor, krävs då att de supersymmetriska partiklarnas massor inte är alltför stora; de borde vara högst kring tusen protonmassor. Det finns också andra idéer om hur man skulle kunna kringgå problemen med Higgsmassan, men gemensamt för alla sådana teorier är att de uppvisar nya partiklar med massor under tusen protonmassor, partiklar som kommer att kunna upptäckas vid *LHC*.

LHC och nya partiklar

LHC, vilket står för *Large Hadron Collider*, är en 27 km lång proton-accelerator som just nu håller på att byggas i den tunnel där tidigare LEP-acceleratorn fanns på CERN utanför Genève. Detta är ett enormt projekt, som inkluderar tusentals partikelfysiker från hela världen. Vid LHC kommer man att återskapa en miljö som inte existerat sedan en bråkdel sekund efter Big Bang, ursmällen vid universums skapelse. Där kommer man (med största sannolikhet) att kunna se hur man ska utvidga Standardmodellen. De energier man kommer upp till i LHC kommer nämligen att motsvara 14000 protonmassor, vilket innebär att det finns gott

om energi för att skapa partiklar med massor under tusen protonmassor. Det är emellertid oerhört komplicerat att urskilja ny fysik vid LHC, eftersom dessa nya, tunga partiklar är extremt kortlivade och snabbt sönderfaller till vanliga Standardmodellpartiklar. Det kommer också att skapas enorma mängder vanliga partiklar vid kollisionerna, och man måste därför vara mycket noggrann för att kunna urskilja den nya fysiken från denna nästan ogenomträngliga bakgrund.

Det andra projekt som jag har arbetat med (artiklarna V-VII) handlar om att förbättra förutsägelsena för hur man ska kunna hitta en typ av partikel som kallas *laddad Higgspartikel* (eller *Higgsboson*) och är en elektriskt laddad kusin till den vanligen neutrala Higgspartikeln. Denna partikel förutsägs i såväl supersymmetri som andra utvidgningar av Standardmodellen. Eftersom det inte finns någon liknande partikel i den vanliga Standardmodellen, vore det ett tydligt tecken på ny fysik om man skulle hitta en sådan vid LHC. Genom att undersöka hur den förhåller sig till andra partiklar i fråga om massa och växelverknningar kommer man också kunna säga något om vilken typ av ny fysik det är som vi ser.

De viktigaste produktionsprocesserna för laddade Higgspartiklar är då den produceras tillsammans med en topp- och en botten-kvark (se figur 6.2). Vi har utvecklat en metod för att kombinera de två av dessa processer som är dominerande, på ett sådant sätt att vi undviker dubbelräkning av bidrag till produktionen. Därmed har vi åstadkommit en beskrivning av produktionen av laddade Higgspartiklar som fungerar oavsett vilka riktningar och hastigheter partiklarna har.

Båda de projekt jag har jobbat med har alltså handlat om att på olika sätt förbättra vår förståelse av hur världen fungerar på dess mest fundamentala nivåer.

Acknowledgements

I would first and foremost like to thank my supervisor, Gunnar Ingelman, for his help, support and many wisdoms concerning physics and life as a scientist, and for giving me the opportunity to see the world through summer schools and conferences. My second supervisor, Johan Rathsman, is no less worthy of gratitude, for his scientific excellence and good research ideas, and for his critical but kind eye.

Next I would like to thank the Theoretical High Energy Physics group graduate students: Nicusor, Rikard and not least David, for all the help and tutoring in the practical tools of the trade, for many interesting discussions on more or less serious topics, and for good friendship. The latter extends to our diploma students Magdalena and Korinna and our postdoc Stefan as well.

A great thank you to the whole department of Radiation Sciences for giving me a nice environment for my PhD studies. Special thanks to my graduate student colleagues Mattias, Agnes, Karin, Örjan, Henrik, Nils and Bjarte. I also want to mention Inger Ericson, for taking care of all practicalities whenever they arise, and Ib Koersner for his ever cheerful help with computer-based problems. And not least, thanks to the Graduate programme in physics and astronomy at Uppsala University, gradU, for financing my PhD position.

Then there are of course all my friends in Uppsala who have made my time here so enjoyable: Patrik, Jöns, Henrik and Rosemary, Miklos and Kristina, Shirin and Markus, Tom, Jörgen, Mats, Josef, and everybody in Glansbandet. Stay in touch! Special thanks also to Niclas, for physics, music and Takéa, to Conny, for introducing me to the joy of heavy metal and motorcycling, and to Klas, for being my oldest friend.

Finally, I want to thank my wife, Jenny, and my large and wonderful family, including my parents-in-law and Malla. Thank you all! I love you!

Bibliography

- [1] F. Mandl and G. Shaw, *Quantum field theory*. Chichester, UK: Wiley (1984) 354 p. (A Wiley-interscience Publication).
- [2] F. Gross, *Relativistic quantum mechanics and field theory*. New York, USA: Wiley (1993) 629 p.
- [3] T. P. Cheng and L. F. Li, *Gauge theory of elementary particle physics*. Oxford, UK: Clarendon (1984) 536 p. (Oxford Science Publications).
- [4] H. Weyl, "Electron and gravitation," *Z. Phys.* **56** (1929) 330–352.
- [5] C.-N. Yang and R. L. Mills, "Conservation of isotopic spin and isotopic gauge invariance," *Phys. Rev.* **96** (1954) 191–195.
- [6] S. L. Glashow, "Partial symmetries of weak interactions," *Nucl. Phys.* **22** (1961) 579–588.
- [7] S. Weinberg, "A model of leptons," *Phys. Rev. Lett.* **19** (1967) 1264–1266.
- [8] A. Salam, "Weak and electromagnetic interactions." In *Svartholm: Elementary particle theory, proceedings of the Nobel Symposium held 1968 at Lerum, Sweden*, Stockholm 1968, 367–377.
- [9] G. 't Hooft, "Renormalization of massless Yang-Mills fields," *Nucl. Phys.* **B33** (1971) 173–199.
G. 't Hooft, "Renormalizable Lagrangians for massive Yang-Mills fields," *Nucl. Phys.* **B35** (1971) 167–188.
- [10] Y. Nambu, "Axial vector current conservation in weak interactions," *Phys. Rev. Lett.* **4** (1960) 380–382.
- [11] J. Goldstone, "Field theories with 'superconductor' solutions," *Nuovo Cim.* **19** (1961) 154–164.
- [12] P. W. Higgs, "Broken symmetries, massless particles and gauge fields," *Phys. Lett.* **12** (1964) 132–133.
P. W. Higgs, "Spontaneous symmetry breakdown without massless bosons," *Phys. Rev.* **145** (1966) 1156–1163.

- [13] **LEP** Collaboration, “A combination of preliminary electroweak measurements and constraints on the standard model,” [hep-ex/0412015](https://arxiv.org/abs/hep-ex/0412015).
- [14] **Particle Data Group** Collaboration, S. Eidelman *et al.*, “Review of particle physics,” *Phys. Lett.* **B592** (2004) 1.
- [15] G. Altarelli, “The electroweak interactions in the standard model and beyond,” [hep-ph/0406270](https://arxiv.org/abs/hep-ph/0406270).
 G. Altarelli, “Status of the standard model and beyond,” *Nucl. Instrum. Meth.* **A518** (2004) 1–8, [hep-ph/0306055](https://arxiv.org/abs/hep-ph/0306055).
 G. Altarelli, “Status of the standard model and beyond,”. Prepared for 6th Hellenic School and Workshop on Elementary Particle Physics, Corfu, Greece, 6-26 Sep 1998.
- [16] **UA1** Collaboration, G. Arnison *et al.*, “Experimental observation of lepton pairs of invariant mass around 95-GeV/c**2 at the CERN SPS collider,” *Phys. Lett.* **B126** (1983) 398–410.
UA2 Collaboration, P. Bagnaia *et al.*, “Evidence for $Z^0 \rightarrow e^+ e^-$ at the CERN anti-p p collider,” *Phys. Lett.* **B129** (1983) 130–140.
UA1 Collaboration, G. Arnison *et al.*, “Experimental observation of isolated large transverse energy electrons with associated missing energy at $s^{**}(1/2) = 540\text{-GeV}$,” *Phys. Lett.* **B122** (1983) 103–116.
UA2 Collaboration, M. Banner *et al.*, “Observation of single isolated electrons of high transverse momentum in events with missing transverse energy at the CERN anti-p p collider,” *Phys. Lett.* **B122** (1983) 476–485.
- [17] D. Schaile, “Precision tests of the electroweak interaction.” Talk given at 27th International Conference on High Energy Physics (ICHEP), Glasgow, Scotland, 20-27 Jul 1994.
- [18] **CDF** Collaboration, F. Abe *et al.*, “Observation of top quark production in anti-p p collisions,” *Phys. Rev. Lett.* **74** (1995) 2626–2631, [hep-ex/9503002](https://arxiv.org/abs/hep-ex/9503002).
D0 Collaboration, S. Abachi *et al.*, “Observation of the top quark,” *Phys. Rev. Lett.* **74** (1995) 2632–2637, [hep-ex/9503003](https://arxiv.org/abs/hep-ex/9503003).
- [19] C. Diaconu, “Electroweak measurements.” Talk given at the XXII International Symposium on Lepton-Photon Interactions at High Energy, Uppsala, Sweden, 30 June-5 July 2005.
- [20] **ALEPH** Collaboration, R. Barate *et al.*, “Search for the standard model Higgs boson at LEP,” *Phys. Lett.* **B565** (2003) 61–75, [hep-ex/0306033](https://arxiv.org/abs/hep-ex/0306033).

- [21] C. F. Kolda and H. Murayama, “The Higgs mass and new physics scales in the minimal standard model,” *JHEP* **07** (2000) 035, [hep-ph/0003170](#).
- [22] W. J. Marciano, G. Valencia, and S. Willenbrock, “Renormalization group improved unitarity bounds on the Higgs boson and top quark masses,” *Phys. Rev.* **D40** (1989) 1725.
B. W. Lee, C. Quigg, and H. B. Thacker, “Weak interactions at very high-energies: The role of the Higgs boson mass,” *Phys. Rev.* **D16** (1977) 1519.
- [23] G. 't Hooft, “Naturalness, chiral symmetry, and spontaneous chiral symmetry breaking.” Lecture given at Cargese Summer Inst., Cargese, France, Aug 26 - Sep 8, 1979.
- [24] H. Georgi and S. L. Glashow, “Unity of all elementary particle forces,” *Phys. Rev. Lett.* **32** (1974) 438–441.
- [25] U. Amaldi, W. de Boer, and H. Furstenau, “Comparison of grand unified theories with electroweak and strong coupling constants measured at LEP,” *Phys. Lett.* **B260** (1991) 447–455.
- [26] J. R. Ellis, “Beyond the standard model for hillwalkers,” [hep-ph/9812235](#).
- [27] **WMAP** Collaboration, D. N. Spergel *et al.*, “First year Wilkinson microwave anisotropy probe (WMAP) observations: Determination of cosmological parameters,” *Astrophys. J. Suppl.* **148** (2003) 175, [astro-ph/0302209](#).
- [28] **SNO** Collaboration, Q. R. Ahmad *et al.*, “Measurement of the charged current interactions produced by B-8 solar neutrinos at the Sudbury Neutrino Observatory,” *Phys. Rev. Lett.* **87** (2001) 071301, [nucl-ex/0106015](#).
- [29] R. Barbieri and A. Strumia, “What is the limit on the Higgs mass?,” *Phys. Lett.* **B462** (1999) 144–149, [hep-ph/9905281](#).
- [30] M. Schmaltz and D. Tucker-Smith, “Little Higgs review,” [hep-ph/0502182](#).
- [31] R. K. Kaul, “Technicolor,” *Rev. Mod. Phys.* **55** (1983) 449.
C. T. Hill and E. H. Simmons, “Strong dynamics and electroweak symmetry breaking,” *Phys. Rept.* **381** (2003) 235–402, [hep-ph/0203079](#).
- [32] C. Csaki, “Higgsless electroweak symmetry breaking,” [hep-ph/0412339](#).
- [33] N. Arkani-Hamed, S. Dimopoulos, and G. R. Dvali, “The hierarchy problem and new dimensions at a millimeter,” *Phys. Lett.* **B429** (1998) 263–272, [hep-ph/9803315](#).
L. Randall and R. Sundrum, “A large mass hierarchy from a small extra dimension,” *Phys. Rev. Lett.* **83** (1999) 3370–3373, [hep-ph/9905221](#).

- [34] **DELPHI** Collaboration, “Search for charged Higgs bosons at LEP in general two Higgs doublet models,” *Eur. Phys. J.* **C34** (2004) 399–418, [hep-ex/0404012](https://arxiv.org/abs/hep-ex/0404012).
- [35] J. R. Ellis, J. S. Hagelin, D. V. Nanopoulos, and M. Srednicki, “Search for supersymmetry at the anti-p p collider,” *Phys. Lett.* **B127** (1983) 233.
- [36] S. Weinberg, *The quantum theory of fields. Vol. 3: Supersymmetry*. Cambridge, UK: Univ. Press (2000) 419 p.
- [37] J. Wess and J. Bagger, *Supersymmetry and supergravity*. Princeton, USA: Univ. Press (1992) 259 p.
D. Bailin and A. Love, *Supersymmetric gauge field theory and string theory*. Bristol, UK: IOP (1994) 322 p. (Graduate student series in physics).
- [38] S. Dawson, “SUSY and such,” [hep-ph/9612229](https://arxiv.org/abs/hep-ph/9612229).
J. Alwall, “Supersymmetry and extensions of the Standard Model.” M.Sc. thesis, Uppsala university, UPTec F 00 078 (2000). Available from <http://www.teorfys.uu.se/COURSES/exjobb/susy.pdf>.
- [39] J. Wess and B. Zumino, “Supergauge transformations in four-dimensions,” *Nucl. Phys.* **B70** (1974) 39–50.
- [40] R. Haag, J. T. Lopuszanski, and M. Sohnius, “All possible generators of supersymmetries of the S matrix,” *Nucl. Phys.* **B88** (1975) 257.
- [41] L. Girardello and M. T. Grisaru, “Soft breaking of supersymmetry,” *Nucl. Phys.* **B194** (1982) 65.
- [42] P. Fayet, “Supergauge invariant extension of the Higgs mechanism and a model for the electron and its neutrino,” *Nucl. Phys.* **B90** (1975) 104–124.
- [43] S. Profumo and C. E. Yaguna, “A statistical analysis of supersymmetric dark matter in the MSSM after WMAP,” *Phys. Rev.* **D70** (2004) 095004, [hep-ph/0407036](https://arxiv.org/abs/hep-ph/0407036).
- [44] S. Dimopoulos and H. Georgi, “Softly broken supersymmetry and SU(5),” *Nucl. Phys.* **B193** (1981) 150.
- [45] S. Dimopoulos and D. W. Sutter, “The supersymmetric flavor problem,” *Nucl. Phys.* **B452** (1995) 496–512, [hep-ph/9504415](https://arxiv.org/abs/hep-ph/9504415).
- [46] G. L. Kane, C. F. Kolda, L. Roszkowski, and J. D. Wells, “Study of constrained minimal supersymmetry,” *Phys. Rev.* **D49** (1994) 6173–6210, [hep-ph/9312272](https://arxiv.org/abs/hep-ph/9312272).

- [47] G. F. Giudice and R. Rattazzi, “Theories with gauge-mediated supersymmetry breaking,” *Phys. Rept.* **322** (1999) 419–499, [hep-ph/9801271](#).
- [48] L. Randall and R. Sundrum, “Out of this world supersymmetry breaking,” *Nucl. Phys.* **B557** (1999) 79–118, [hep-th/9810155](#).
- [49] J. R. Espinosa and R.-J. Zhang, “Complete two-loop dominant corrections to the mass of the lightest CP-even Higgs boson in the minimal supersymmetric standard model,” *Nucl. Phys.* **B586** (2000) 3–38, [hep-ph/0003246](#).
- [50] J. F. Gunion, H. E. Haber, G. L. Kane, and S. Dawson, *The Higgs Hunter’s Guide*. Perseus Books, Frontiers in Physics Vol. 80 (1990) 423 p.
- [51] S. Davidson and H. E. Haber, “Basis-independent methods for the two-Higgs-doublet model,” [hep-ph/0504050](#).
- [52] S. L. Glashow and S. Weinberg, “Natural conservation laws for neutral currents,” *Phys. Rev.* **D15** (1977) 1958.
- [53] S. Moretti and J. Rathsman, “Pair production of charged Higgs bosons in association with bottom quark pairs at the Large Hadron Collider,” *Eur. Phys. J.* **C33** (2004) 41–52, [hep-ph/0308215](#).
- [54] A. G. Akeroyd, A. Arhrib, and E.-M. Naimi, “Note on tree-level unitarity in the general two Higgs doublet model,” *Phys. Lett.* **B490** (2000) 119–124, [hep-ph/0006035](#).
- [55] M. Gell-Mann, “A schematic model of baryons and mesons,” *Phys. Lett.* **8** (1964) 214–215.
- [56] G. Zweig, “An SU(3) model for strong interaction symmetry and its breaking. 2.” CERN-TH-412.
- [57] M. Y. Han and Y. Nambu, “Three-triplet model with double SU(3) symmetry,” *Phys. Rev.* **139** (1965) B1006–B1010.
M. Gell-Mann, “Quarks,” *Acta Phys. Austriaca Suppl.* **9** (1972) 733–761.
- [58] D. J. Gross and F. Wilczek, “Ultraviolet behavior of non-Abelian gauge theories,” *Phys. Rev. Lett.* **30** (1973) 1343–1346.
H. D. Politzer, “Reliable perturbative results for strong interactions?,” *Phys. Rev. Lett.* **30** (1973) 1346–1349.
- [59] S. Scherer, “Introduction to chiral perturbation theory,” [hep-ph/0210398](#).
- [60] J. Smit, *Introduction to quantum fields on a lattice: A robust mate*. Cambridge Lect. Notes Phys., Vol. 15 (2002) 271 p.

- [61] K. I. Ishikawa, “Hadron spectrum from dynamical lattice QCD simulations,” *Nucl. Phys. Proc. Suppl.* **140** (2005) 20–33, [hep-lat/0410050](#).
- [62] M. Luscher, “Lattice QCD: From quark confinement to asymptotic freedom,” *Annales Henri Poincare* **4** (2003) S197–S210, [hep-ph/0211220](#).
- [63] T. Muta, *Foundations of Quantum Chromodynamics. Second edition.* World Sci. Lect. Notes Phys., Vol. 57 (1998) 409 p.
- [64] G. 't Hooft and M. J. G. Veltman, “Regularization and renormalization of gauge fields,” *Nucl. Phys.* **B44** (1972) 189–213.
- [65] L. D. Landau, A. Abrikosov, and L. Halatnikov, “On the quantum theory of fields,” *Nuovo Cim. Suppl.* **3** (1956) 80–104.
- [66] S. Bethke, “Determination of the QCD coupling $\alpha(s)$,” *J. Phys.* **G26** (2000) R27, [hep-ex/0004021](#).
- [67] S. J. Brodsky, S. Menke, C. Merino, and J. Rathsmann, “On the behavior of the effective QCD coupling $\alpha(\tau)(s)$ at low scales,” *Phys. Rev.* **D67** (2003) 055008, [hep-ph/0212078](#).
- [68] S. Bethke, “ $\alpha(s)$ at Zinnowitz 2004,” *Nucl. Phys. Proc. Suppl.* **135** (2004) 345–352, [hep-ex/0407021](#).
- [69] T. van Ritbergen, J. A. M. Vermaseren, and S. A. Larin, “The four-loop beta function in quantum chromodynamics,” *Phys. Lett.* **B400** (1997) 379–384, [hep-ph/9701390](#).
- [70] R. K. Ellis, W. J. Stirling, and B. R. Webber, *QCD and collider physics.* Camb. Monogr. Part. Phys. Nucl. Phys. Cosmol., Vol. 8 (1996) 435 p.
- [71] J. Callan, Curtis G. and D. J. Gross, “High-energy electroproduction and the constitution of the electric current,” *Phys. Rev. Lett.* **22** (1969) 156–159.
- [72] J. D. Bjorken, “Asymptotic sum rules at infinite momentum,” *Phys. Rev.* **179** (1969) 1547–1553.
- [73] G. Miller *et al.*, “Inelastic electron - proton scattering at large momentum transfers,” *Phys. Rev.* **D5** (1972) 528.
- [74] W. A. Bardeen, A. J. Buras, D. W. Duke, and T. Muta, “Deep inelastic scattering beyond the leading order in asymptotically free gauge theories,” *Phys. Rev.* **D18** (1978) 3998.
- [75] M. E. Peskin and D. V. Schroeder, *An introduction to quantum field theory.* Reading, USA: Addison-Wesley (1995) 842 p.

- [76] V. N. Gribov and L. N. Lipatov, “Deep inelastic e p scattering in perturbation theory,” *Sov. J. Nucl. Phys.* **15** (1972) 438–450.
G. Altarelli and G. Parisi, “Asymptotic freedom in parton language,” *Nucl. Phys.* **B126** (1977) 298.
Y. L. Dokshitzer, “Calculation of the structure functions for deep inelastic scattering and e+ e- annihilation by perturbation theory in Quantum Chromodynamics. (in russian),” *Sov. Phys. JETP* **46** (1977) 641–653.
- [77] S. J. Brodsky and G. R. Farrar, “Scaling laws for large momentum transfer processes,” *Phys. Rev.* **D11** (1975) 1309.
- [78] V. S. Fadin, E. A. Kuraev, and L. N. Lipatov, “On the Pomeranchuk singularity in asymptotically free theories,” *Phys. Lett.* **B60** (1975) 50–52.
I. I. Balitsky and L. N. Lipatov, “The Pomeranchuk singularity in quantum chromodynamics,” *Sov. J. Nucl. Phys.* **28** (1978) 822–829.
- [79] A. Vogt, S. Moch, and J. A. M. Vermaseren, “The three-loop splitting functions in QCD: The singlet case,” *Nucl. Phys.* **B691** (2004) 129–181, [hep-ph/0404111](https://arxiv.org/abs/hep-ph/0404111).
S. Moch, J. A. M. Vermaseren, and A. Vogt, “The three-loop splitting functions in QCD: The non-singlet case,” *Nucl. Phys.* **B688** (2004) 101–134, [hep-ph/0403192](https://arxiv.org/abs/hep-ph/0403192).
- [80] T. Sjöstrand, L. Lönnblad, S. Mrenna, and P. Skands, “Pythia 6.3: Physics and manual,” [hep-ph/0308153](https://arxiv.org/abs/hep-ph/0308153).
- [81] A. A. Bhatti, “Inclusive jet production at Tevatron.” Presented at 10th Topical Workshop on Proton-Antiproton Collider Physics, Batavia, IL, 9-13 May 1995.
CDF Collaboration, F. Abe *et al.*, “Inclusive jet cross section in $\bar{p}p$ collisions at $\sqrt{s} = 1.8$ TeV,” *Phys. Rev. Lett.* **77** (1996) 438–443, [hep-ex/9601008](https://arxiv.org/abs/hep-ex/9601008).
- [82] J. Huston *et al.*, “Large transverse momentum jet production and the gluon distribution inside the proton,” *Phys. Rev. Lett.* **77** (1996) 444–447, [hep-ph/9511386](https://arxiv.org/abs/hep-ph/9511386).
A. D. Martin, R. G. Roberts, and W. J. Stirling, “Parton distributions: A study of the new HERA data, alpha(s), the gluon and p anti-p jet production,” *Phys. Lett.* **B387** (1996) 419–426, [hep-ph/9606345](https://arxiv.org/abs/hep-ph/9606345).
- [83] J. Pumplin *et al.*, “New generation of parton distributions with uncertainties from global QCD analysis,” *JHEP* **07** (2002) 012, [hep-ph/0201195](https://arxiv.org/abs/hep-ph/0201195).
- [84] M. Gluck, E. Reya, and A. Vogt, “Parton distributions for high-energy collisions,” *Z. Phys.* **C53** (1992) 127–134.

- [85] J. G. H. de Groot *et al.*, “Inclusive interactions of high-energy neutrinos and anti-neutrinos in iron,” *Z. Phys.* **C1** (1979) 143.
H. Abramowicz *et al.*, “Experimental study of opposite sign dimuons produced in neutrino and anti-neutrinos interactions,” *Z. Phys.* **C15** (1982) 19.
- [86] A. S. Ito *et al.*, “Measurement of the continuum of dimuons produced in high-energy proton - nucleus collisions,” *Phys. Rev.* **D23** (1981) 604.
- [87] R. D. Field and R. P. Feynman, “Quark elastic scattering as a source of high transverse momentum mesons,” *Phys. Rev.* **D15** (1977) 2590–2616.
- [88] R. Vogt, “Physics of the nucleon sea quark distributions,” *Prog. Part. Nucl. Phys.* **45** (2000) S105–S169, [hep-ph/0011298](https://arxiv.org/abs/hep-ph/0011298).
- [89] A. Edin and G. Ingelman, “A model for the parton distributions in hadrons,” *Phys. Lett.* **B432** (1998) 402–410, [hep-ph/9803496](https://arxiv.org/abs/hep-ph/9803496).
- [90] B. Andersson, G. Gustafson, G. Ingelman, and T. Sjöstrand, “Parton fragmentation and string dynamics,” *Phys. Rept.* **97** (1983) 31.
- [91] B. R. Webber, “A QCD model for jet fragmentation including soft gluon interference,” *Nucl. Phys.* **B238** (1984) 492.
- [92] G. Corcella *et al.*, “Herwig 6: An event generator for hadron emission reactions with interfering gluons (including supersymmetric processes),” *JHEP* **01** (2001) 010, [hep-ph/0011363](https://arxiv.org/abs/hep-ph/0011363).
- [93] S. Mandelstam, “Determination of the pion-nucleon scattering amplitude from dispersion relations and unitarity. General theory,” *Phys. Rev.* **112** (1958) 1344–1360.
- [94] A. C. Irving and R. P. Worden, “Regge phenomenology,” *Phys. Rept.* **34** (1977) 117–231.
- [95] A. Donnachie and P. V. Landshoff, “Total cross-sections,” *Phys. Lett.* **B296** (1992) 227–232, [hep-ph/9209205](https://arxiv.org/abs/hep-ph/9209205).
- [96] J. Sakurai, *Modern Quantum Mechanics, Revised Edition*. Reading, Mass.: Addison-Wesley (1994) 500 p.
- [97] T. H. Bauer, R. D. Spital, D. R. Yennie, and F. M. Pipkin, “The hadronic properties of the photon in high-energy interactions,” *Rev. Mod. Phys.* **50** (1978) 261.
- [98] J. J. Sakurai and D. Schildknecht, “Generalized vector dominance and inelastic electron - proton scattering,” *Phys. Lett.* **B40** (1972) 121–126.

- [99] G. Cvetič, D. Schildknecht, and A. Shoshi, “Deep inelastic scattering, QCD, and generalized vector dominance,” *Eur. Phys. J.* **C13** (2000) 301–314, [hep-ph/9908473](#).
- [100] **NuTeV** Collaboration, D. A. Harris *et al.*, “Precision calibration of the NuTeV calorimeter,” *Nucl. Instrum. Meth.* **A447** (2000) 377–415, [hep-ex/9908056](#).
- [101] E. A. Paschos and L. Wolfenstein, “Tests for neutral currents in neutrino reactions,” *Phys. Rev.* **D7** (1973) 91–95.
- [102] **NuTeV** Collaboration, G. P. Zeller *et al.*, “A precise determination of electroweak parameters in neutrino nucleon scattering,” *Phys. Rev. Lett.* **88** (2002) 091802, [hep-ex/0110059](#).
- [103] G. P. Zeller, “Summary of work on possible NuTeV explanations.” Web page at <http://home.fnal.gov/~gzeller/nutev.html>.
- [104] S. Davidson, S. Forte, P. Gambino, N. Rius, and A. Strumia, “Old and new physics interpretations of the NuTeV anomaly,” *JHEP* **02** (2002) 037, [hep-ph/0112302](#).
- [105] D. Mason, “NuTeV Strange/Antistrange Sea Measurements from Neutrino Charm Production.” To be published in the proceedings of the XIII International Workshop on Deep Inelastic Scattering, Madison, Wisconsin, 27 April-1 May 2005.
- [106] A. D. Martin, R. G. Roberts, W. J. Stirling, and R. S. Thorne, “Parton distributions incorporating QED contributions,” *Eur. Phys. J.* **C39** (2005) 155–161, [hep-ph/0411040](#).
- [107] “LHC - The Large Hadron Collider.” Web page at <http://www.cern.ch/lhc>.
- [108] F. Gianotti, “Probing the hierarchy problem with the LHC.” Talk given at the XXII International Symposium on Lepton-Photon Interactions at High Energy, Uppsala, Sweden, 30 June-5 July 2005.
- [109] A. D. Martin, R. G. Roberts, W. J. Stirling, and R. S. Thorne, “Uncertainties of predictions from parton distributions. I: Experimental errors,” *Eur. Phys. J.* **C28** (2003) 455–473, [hep-ph/0211080](#).
- [110] D. Stump *et al.*, “Inclusive jet production, parton distributions, and the search for new physics,” *JHEP* **10** (2003) 046, [hep-ph/0303013](#).

- [111] A. D. Martin, R. G. Roberts, W. J. Stirling, and R. S. Thorne, “Uncertainties of predictions from parton distributions. II: Theoretical errors,” *Eur. Phys. J.* **C35** (2004) 325–348, [hep-ph/0308087](#).
- [112] J. Huston, J. Pumplin, D. Stump, and W. K. Tung, “Stability of NLO global analysis and implications for hadron collider physics,” [hep-ph/0502080](#).
- [113] S. Catani, F. Krauss, R. Kuhn, and B. R. Webber, “QCD matrix elements + parton showers,” *JHEP* **11** (2001) 063, [hep-ph/0109231](#).
F. Krauss, “Matrix elements and parton showers in hadronic interactions,” *JHEP* **08** (2002) 015, [hep-ph/0205283](#).
- [114] S. J. Brodsky, G. P. Lepage, and P. B. Mackenzie, “On the elimination of scale ambiguities in perturbative quantum chromodynamics,” *Phys. Rev.* **D28** (1983) 228.
G. Ingelman and J. Rathsman, “Renormalization scale uncertainty in the DIS (2+1) jet cross-section,” *Z. Phys.* **C63** (1994) 589–600, [hep-ph/9405367](#).